We are IntechOpen, the world's leading publisher of Open Access books Built by scientists, for scientists

6,900
Open access books available

185,000
International authors and editors

200M
Downloads

Our authors are among the

154
Countries delivered to

TOP 1%
most cited scientists

12.2%
Contributors from top 500 universities



WEB OF SCIENCE™

Selection of our books indexed in the Book Citation Index in Web of Science™ Core Collection (BKCI)

Interested in publishing with us?
Contact book.department@intechopen.com

Numbers displayed above are based on latest data collected.
For more information visit www.intechopen.com



6

Electronic Transport in an NS System With a Pure Normal Channel. Coherent and Spin-Dependent Effects

Yu. N. Chiang (Tszyan)
B.Verkin Institute for Low Temperature Physics and Engineering, National Academy of Sciences of Ukraine, Kharkov 61103
Ukraine

1. Introduction

The proved possibility really to observe quantum-interference phenomena in metals of various purity, in conditions when the scattering occurs mainly at static defects and the electron mean free path, l_{el}, is much less than the size L of the investigated sample, convinces that the phase φ of electron wave functions does not break down at elastic (without changing electron energy) scattering. Even in very pure metals with $l_{el} \approx 0.1$ mm, at $T \leq 4$ K, collisions of electrons with phonons occur much less frequently than those with static defects occur, so that the role of the former in electron kinetics becomes minor. In other words, the inequality $L_\varphi > l_{el}$ is usually satisfied in a metal at sufficiently low temperatures, where L_φ is the phase-breaking length. This condition, however, is not sufficient to observe coherent phenomena. For example, the phenomena of interference nature such as the oscillations in conductance in a magnetic flux ϕ in normal - metal systems (Sharvin & Sharvin, 1981) or coherent effects in hybrid systems "normal metal/superconductor" (NS) (Lambert & Raimondi, 1998), can become apparent given certain additional relations are fulfilled between the parameters, which define the level of the effects: $l_{el} \leq L \leq \xi_T \leq L_\varphi$. Here, ξ_T is the thermal coherence length. Otherwise, at reverse inequalities, a fraction of the coherent phenomena in total current is expected to be exponentially small. It follows from the general expression for the phase-sensitive current: $J(\phi) \sim F(\phi)(l_{el}/L)\exp(-L/\xi_T)\exp(-L_\varphi/\xi_T)$ ($F(\phi)$ is a periodic function).

The majority of coherent effects, as is known, is realized in experiments on mesoscopic systems with typical parameters $L \sim 1$ μm $\gg l_{el} \sim 0.01$ μm, i. e., under conditions where the level of the effects is exponentially small, but still supposed to be detected (Lambert & Raimondi, 1998; Washburn & Webb, 1986). Really, the maximum possible (in the absence of scattering) spatial coherence length, ξ_0, according to the indeterminacy principle, is of the order of $\xi_0 = (\hbar v_F/k_B T) \sim 1$ μm in value, for a pair of single-particle excitations in a normal metal (for example, for $e-h$ hybrids resulting from the Andreev reflection (Andreev, 1964)). That value is the same as a typical size of mesoscopic systems. As a consequence, from the ratio $\xi_T \sim \sqrt{(1/3)\xi_0 l_{el}}$ it follows that in these systems, coherent effects are always realized under conditions $L \gg \xi_T \gg l_{el}$ and are exponentially small on the L scale.

From the above typical relations between the basic microscopic parameters in mesoscopic systems one can see that such systems cannot give an idea about a true scale of the most important parameter - the phase-breaking length L_φ for electron wave functions. It is only possible to say that its value is greater than $L \sim 1$ μm. In mesoscopic systems, a value of the thermal coherence length ξ_T remains not quite clear as well, since, under strong inequality $\xi_T \gg l_{el}$, the scale of this parameter should be additionally restricted: At high frequency of elastic scattering processes on impurity centers (at short l_{el}), the portion of inelastic scattering on the same impurities, which breaks down a phase of wave functions, should be also significant.

It is clear that due to spatial restrictions, mesoscopic systems are also of little use for experimental investigation of non-local coherent effects; a keen interest in those effects has recently increased in connection with the revival of general interest in non-local quantum phenomena (Hofstetter et al., 2009).

Our approach to the investigation of phase-breaking and coherence lengths in metals is based on an alternative, macroscopical, statement of the experiment. We presume that in order to assess the real spatial scale of the parameters L_φ, ξ_T, and ξ_0 in metals, the preference should be given to studying coherent effects, first, in pure systems, where the contribution from inelastic scattering processes is minimized due to the lowered concentration of impurities, and, second, at such sizes of systems, which would certainly surpass physically reasonable limiting scales of the specified spatial parameters. The listed requirements mean holding the following chain of inequalities: $L > L_\varphi > l_{el} \gg \xi_0$ ($l_{el}/\xi_0 \geq 10$). They can be satisfied by increasing the electron mean free path l_{el} and the system size L by several orders of magnitude in comparison with the same quantities for mesoscopic systems.

At first glance, such changing in the above parameters should be accompanied by the same, by several orders, reduction in the value of registered effects. Fortunately, this concerns only normal-metal systems, where coherent effects have a weak-localization origin (Altshuler et al., 1981). The remarkable circumstance is that the value of coherent effects in normal (N) and NS systems can differ by many orders of magnitude in favor of the latter. Thus, oscillation amplitude of the conductance in a magnetic field in a normal-metal ring (the Aharonov - Bohm effect in a weak - localization approach (Altshuler et al., 1981; Washburn & Webb, 1986)) can be m times less than that in a ring of similar geometry with a superconducting segment (NS - ring) due to possible resonant degeneration of transverse modes in the Andreev spectrum arising in the SNS system (Kadigrobov et al., 1995). For example, for mesoscopic rings $m \sim 10^4 \div 10^5$. As it will be shown below, coherent effects in macroscopical formulation of experiments remain, nevertheless, rather small in value, and for their observing, the resolution of a voltage level down to 10^{-11} V is required. Unlike mesoscopic statement of the experiment, it makes special non-standard requirements for measuring technique of such low signals. To satisfy the requirements, we have developed the special superconducting commutator with picovolt sensitivity (Chiang, 1985).

Here, we describe the results of our research of quantum coherent phenomena in NS systems consisting of normal metals with macroscopical electron mean free path and having macroscopical sizes, which fact allows us to regard our statement of the experiment as macroscopical. The phenomena are considered, observed in such systems of different connectivity: for both simply connected and doubly connected geometry.

In Section 2, phase-sensitive quantum effects in the "Andreev conductance" of open and closed macroscopic SNS systems are briefly considered. The open SNS systems contain segments, up to 350 μm in length, made of high-pure ($l_{el} \sim 100$ μm) single-crystal normal metals Cu

and Al which are in contact with In, Sn, and Pb in the superconducting or intermediate state. The phase-sensitive magnetoresistive oscillations are described, with a period equal to the flux quantum $hc/2e$, which were found in hybrid quasi-ballistic doubly connected SNS structures with single-crystal normal segments of macroscopic sizes ($L = 100 \div 500$ μm) and elastic electron mean free path on the same scale. The description of resistive oscillations of a resonance shape for the structure In(S) - Al(N) - In(S) of the similar size is provided. The oscillations undergo a phase inversion (a shift by π) with respect to the phase of the nonresonance oscillations.
In Section 3, the results of studying coherent and spin-dependent effects in the conductance of macroscopic heterosystems "magnetic (Fe, Ni) - superconductor (In)" are presented. The first proof of the possibility of observing, with adequate resolution, the characteristic coherent effect in the conductivity of sufficiently pure ferromagnets was given on the example of nickel. The effect consists in an interference decrease in the conductivity on the scale of the very short coherence length of Andreev $e - h$ hybrids. It was shown that this length did not exceed the coherence length estimated using the semiclassical theory for ferromagnetic metals with high exchange energy. Additional proof was obtained for spin accumulation on F/S interfaces. This accumulation comes from the special features of the Andreev reflection under the conditions of spin polarization of the current in a ferromagnet.
The first observation of the $hc/2e$-oscillations (solid-state analogue of the Aharonov-Bohm effect (Aharonov & Bohm, 1959)) is described in the conductance of a ferromagnet, Ni, as a part of the macroscopical S(In) - F(Ni) - S(In) interferometer ($L^{\mathrm{Ni}} \sim 500$ μm). A physical explanation is offered for the parameters of the oscillations observed. We have found that the oscillation amplitude corresponds to the value of the positive resistive contribution to the resistance from a ferromagnetic layer, several nanometers thick, adjacent to the F/S interface. We have demonstrated that the scale of the proximity effect cannot exceed that thickness. The oscillations observed in a disordered conductor of an SFS system, about 1 mm in length, indicate that the diffusion phase-breaking length is macroscopical in sufficiently pure metals, including ferromagnetic ones, even at not too low helium temperatures. The analysis of the non-local nature of the effect is offered.
Section 4 is the Conclusion.

2. Macroscopical NS systems with a non-magnetic normal-metal segment

While trying to detect possible manifestations of quantum coherent phenomena in conductivity of normal metals, the main results were obtained in experiments on the samples of mesoscopic size under diffusion transport conditions, $L \geq \xi_T \gg l_{el}$. In such case, the contribution from the coherent electrons is exponentially small relative to the averaged contribution from all electrons in all distributions. The portion of coherent electrons can be increased due to weak-localization effect. For example, in a doubly connected sample, so-called self-intersecting coherent trajectory of interfering electrons is artificially organized (Washburn & Webb, 1986). If the length of the loop, L, covering the cavity of the doubly connected system does not exceed the phase-breaking length, L_φ, then introducing a magnetic field into the cavity may lead to a synchronous shift of the phase of wave functions of all electrons. As a result, the conductance of the system, determined by a superposition of these functions, will oscillate periodically in the magnetic field. The amplitude of the oscillations will be defined by the weak-localization contribution from interfering reversible self-intersecting transport trajectories (Aharonov & Bohm, 1959; Sharvin & Sharvin, 1981), and the period will be twice as small as that for the conventional Aharonov-Bohm effect in a

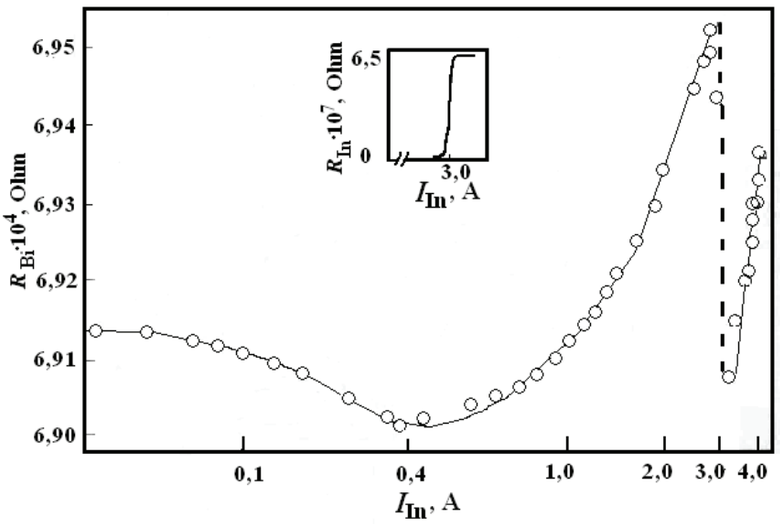


Fig. 1. Positive jump of resistance of bimetallic system Bi/In at converting indium into the superconducting state. Inset: Superconducting transition of In.

normal-metal ring, where the reversibility of the trajectories in the splitted electron beam is not provided.

2.1 Singly connected NS systems

2.1.1 Artificial NS boundary

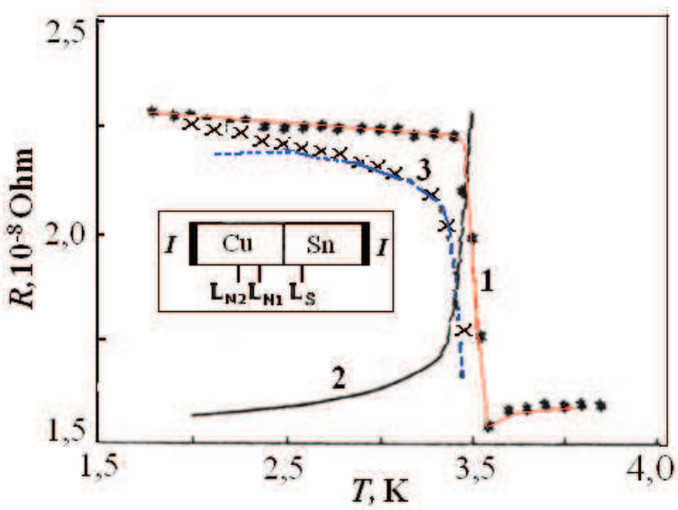


Fig. 2. Positive jump of resistance of bimetallic system Cu/Sn measured on the probes L_{N1}; L_{N2} at converting tin into the superconducting state (curve *1*); calculated portion of the boundary resistance (curve *2*); crosses are experimental points excluding curve *2*; dotted curve *3* is calculated in accordance with Eq. (4). Inset: Schematic view of the sample.

As it has been noted in Introduction, in comparison with weak-localization situation, the role of coherent interference repeatedly increases in the normal metal, which is affected by Andreev reflection - the mechanism naturally generating coherent quasiparticles. In a

hybrid "normal metal/type I superconductor" system (*NS* system), the contribution from the coherent excitations into normal conductivity dominates over the distance scale of the order of a ballistic path from the *NS* boundary ($\sim 1\mu$m), irrespective of the system size, its connectivity, and, generally, the electron mean free path; due to Andreev reflection, the spectrum of coherent excitations is always resolved on this scale. From the discussion in Introduction it clearly follows that in macroscopical statement of experiments, maximum level of the coherent effects should be reached in conditions, where the electron mean free path, l_{el}, the greatest possible coherence length, ξ_0, and the sample length, L (the separation between potential probes), are of the same order of magnitude. In these conditions, when studying even singly connected *NS* systems in 1988, we first revealed an unusual behavior of the normal conductivity of the heterosystem Bi(*N*)/In(*S*) (Chiang & Shevchenko, 1988): The resistance of the area containing the boundary between the two metals unexpectedly decreased rather than increased at the transition of one of the metals (In) from the superconducting into normal state (Fig. 1).

Further theoretical (Herath & Rainer, 1989; Kadigrobov, 1993; Kadigrobov et al., 1995) and our experimental research have shown that the effect is not casual but fundamental. It accompanies diffusive transport of electrons through non-ballistic *NS* contacts. Figure 2 presents some experimental data revealing the specific features of coherent excitation scattering in the vicinity of the *NS* boundaries (see more data in (Chiang & Shevchenko, 1998)) for Cu(*N*)/Sn(*S*) system (schematic view of the sample is shown in the Inset). The basis of the bimetallic *NS* system under investigation was a copper single crystal with a "macroscopically" large elastic mean free path $l_{el}^{N} \simeq 10 - 20$ μm. The single crystal was in contact with a type I superconductor (tin) ($l_{el}^{S} \simeq 100$ μm). The transverse size of contact areas under probes was 20-30 μm so that tunnel properties were not manifested in view of the large area of the junction. Separation of the *N*-probes from the boundary L_{N1}, L_{N2}, and L_S were 13, 45, and 31 μm, respectively. The curve *1* shows a general regularity in the behavior of the resistance of

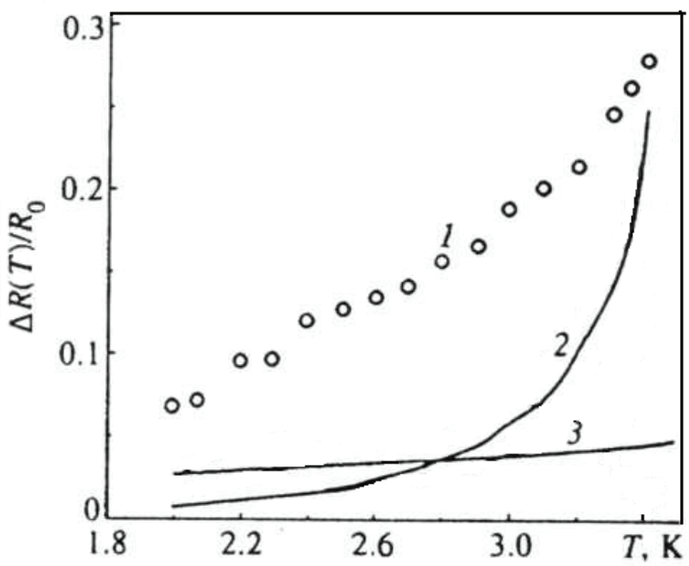


Fig. 3. Resistance of the region of the Cu/In system incorporating the *NS* boundary, below T_c of the superconductor (In): Experimental points (curve *1*) and calculated contributions of the boundary resistance ($z \neq 0$, curve *2*) and of the proximity effect (curve *3*).

normal regions adjoining the common boundary of two contacting metals - occurrence of the positive contribution to the resistance closely related to the temperature dependence of the superconducting gap at transition of one of the metals into the superconducting state. This effect is most pronounced just in the macroscopical statement of experiment in the formulated above optimum conditions $l_{el}^{N} \sim \xi_{0(N)} \sim L_N$.

The considered effect was predicted in (Herath & Rainer, 1989) and (Kadigrobov, 1993). It has been shown that there exists a correction to the normal resistance (hereafter, $\delta R_N^{\mathrm{Andr}}$) leading to an increase in the metal resistance within ballistic distances from the NS boundary upon cooling. The correction may occur due to increased cross section of electron scattering by impurities during multiple interaction of phase-coherent electron and Andreev excitations with impurities and with the NS boundary. According to (Kadigrobov et al., 1995), the relative

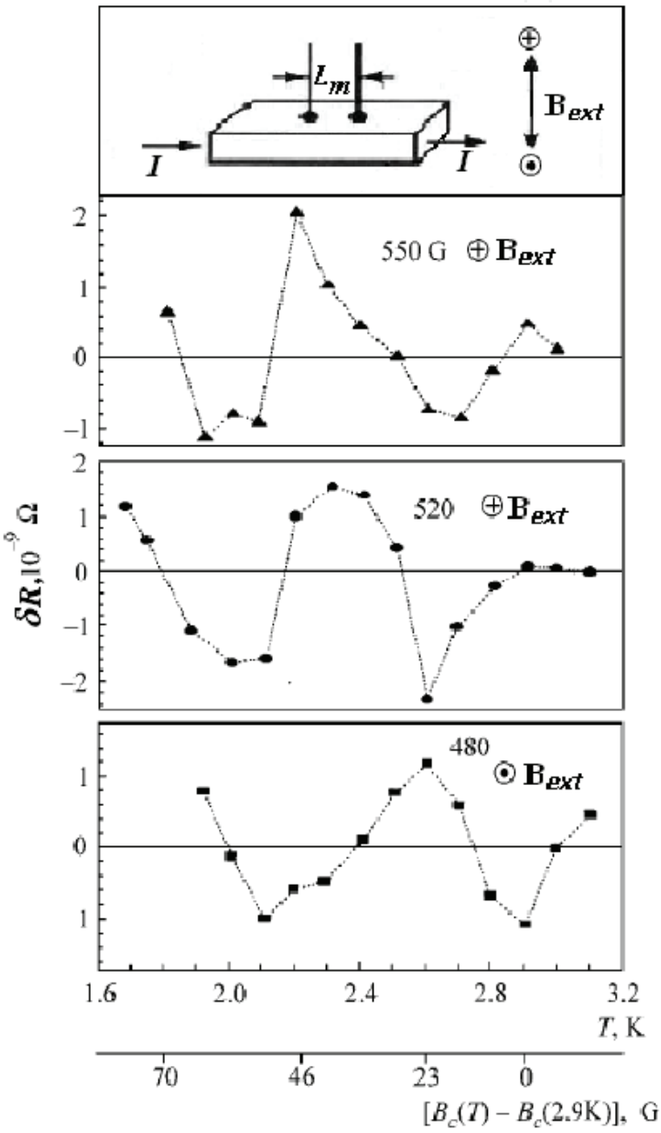


Fig. 4. Temperature $hc/2e$ oscillations of the resistance of the Pb plate (see the outline above) in the intermediate state.

increase in the resistance of a layer, L_N in thickness, measured from the NS boundary and having a resistance R_N prior to the formation of this boundary, should be equal to

$$\frac{\delta R_N^{\text{Andr}}}{R_N} = (l_{el}^N / L_N)\{T_p\}, \tag{1}$$

where $\{T_p\}$ is the effective probability of electron scattering by a layer of thickness of the order of "coherence length" ξ_T taking into account Andreev reflection and the conditions $l_{el}^N \sim \xi_N^* \sim L_N$. The quantity $\{T_p\}$ can be obtained by integrating $T_p = \hbar v_{\text{F}} / \varepsilon l_{el}^N$, viz., the probability that the particle is scattered by an impurity and reflects as an Andreev particle with energy ε (measured from the Fermi level), thus contributing to the resistance over the length l_{el}^N; the integration is over the entire energy range between the minimum energy $\varepsilon_{min} = \hbar v_{\text{F}} / l_{el}^N$ and the maximum energy of the order of the gap energy $\Delta(T)$:

$$\{T_p\} = \int_{\varepsilon_{min}}^{\Delta(T)} (-\frac{\partial f_0}{\partial \varepsilon}) T_p d\varepsilon. \tag{2}$$

Integration to a second approximation gives the following analytical result for the correction to the resistance of the layer L_N under investigation as a function of temperature:

$$\frac{\delta R_N^{\text{Andr}}}{R_N} = \frac{\xi_T}{L_N} F(T), \tag{3}$$

where $F(T)$ is of order of unity with $\xi_T \sim l_{el}^N$. For a pair of probes $(L_{N1}; L_{N2})$ (see Fig. 2) with $L_{N1,2} > l_{el}^N$ it provides

$$\frac{\delta R_{L_{N1};L_{N2}}^{\text{Andr}}}{R_{L_{N1};L_{N2}}} = \frac{\xi_T}{L_{N1} - L_{N2}} \ln(L_{N1}/L_{N2}) F(T). \tag{4}$$

Using Eq. (4) we have estimated the data received for different samples, including those presented in Fig. 2. The analysis reveals not only qualitative but also quantitative agreement between the experiment and the concept of increasing the dissipative scattering contribution due to Andreev reflection (dotted curve *3* in Fig. 2). It is thus important to emphasize once again that optimum conditions for observing this effect are realized by setting measuring probes at a distance of several ballistic coherence lengths ξ_0 from the NS boundary, i. e., in the macroscopical statement of experiment.

Curve *2* in Fig. 2 gives an idea of the portion of the boundary resistance which arises due to dissipative quasiparticle current flowing in the areas close to NS borders, where the order parameter $\Delta = \Delta(x)$ is less than $\Delta(\infty) = 1$. Since the condition $eV \ll k_{\text{B}}T$ was satisfied in our experiment we calculated this curve using the CESST-HC theory (Clarke et al., 1979; Hsiang & Clarke, 1980). In accordance with the theory, the boundary resistance, R_b^{NS}, caused by the potential V_b^{NS} extending into the near-boundary region of a superconductor where $\Delta(x) < 1$, should be of the order of

$$R_b^{\text{NS}} = V_b^{\text{NS}} / I = Y(z,T) R^{\text{Cu}}; \qquad R^{\text{Cu}} = \lambda_Q \cdot \rho^{\text{Cu}} / A, \tag{5}$$

where λ_Q is the distance from the boundary on the side of the superconductor, over which the potential decays that arises from the imbalance between the charges of the pair current and

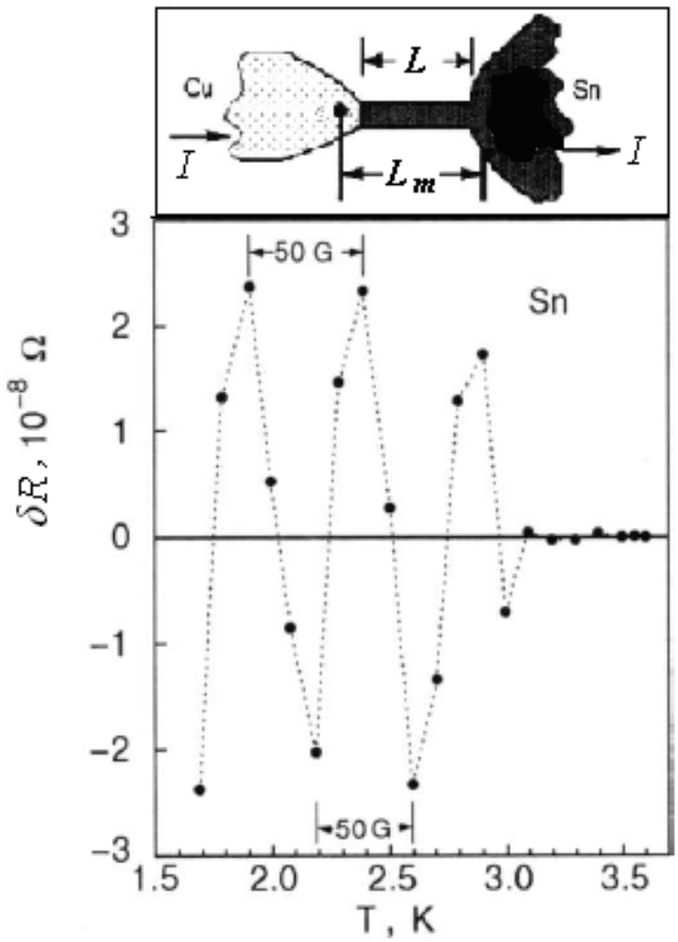


Fig. 5. Temperature $hc/2e$ oscillations of the resistance of the intermediate-state Sn constriction (see the outline above) in a self-current magnetic field of the measuring current $I = 1$ A as the critical magnetic field (50G - intervals are specified).

that of independent quasiparticles; $\rho^{\mathrm{Cu}} = 3/2e^2N(0)l_{el}^{\mathrm{Cu}}v_{\mathrm{F}}$; $N(0)$ is the density of states per spin at the Fermi level, e is the electron charge, v_{F} is the Fermi velocity, and

$$Y(z,T) = (1+z^2)\frac{k_{\mathrm{B}}T}{\Delta}\sqrt{\frac{2\pi\Delta}{k_{\mathrm{B}}T}}\exp(-\Delta/k_{\mathrm{B}}T). \tag{6}$$

Measurements across the probes $L_{N1}; L_S$, with the NS boundary between them and $L_{N1} > l_{el}^{\mathrm{Cu}}$, and estimation of the boundary resistance of Eqs. (5; 6) indicate a manifestation of such coherent transport mechanism, which leads to an increase in conductivity in these non-ballistic conditions (Fig. 3).

According to the Landauer concept (Landauer, 1970), complete thermalization of an electron is the result not of momentum relaxation but of relaxation of the wave function phase due to inelastic scattering in regions with an equilibrium distribution, called "reservoirs" (regions that are sinks and sources of charges). The simulation of a continuous random walk of an elastically scattered particle in a three-dimensional normal layer of the metal showed the need

to consider the trajectories with multiple Andreev reflections. As shown in (Van Wees et al., 1992), the mean diffusional path length $\langle L\rangle$ depends linearly on the width d of the normal layer, where d is the distance between the boundary and the region of equilibrium distribution (reservoir), which is of the order of magnitude of the inelastic mean free path l_{inel}, i. e., $d \sim l_{inel}$. Since the probability τ_r for excitations to pass from the boundary to the reservoir is inversely proportional to the layer width, $\tau_r \sim (l_{el}/d)$, it follows from the linear relation between $\langle L\rangle$ and d that $\langle L\rangle \sim \tau_r^{-1} \propto l_{inel}$.
It is also necessary to take into account the probability of realizing a diffusional trajectory by equating its length to the elastic mean free path, or, equivalently, equating the length $\langle L\rangle \sim \sqrt{\hbar D/k_{\mathrm{B}}T}$ (D is the diffusion coefficient) to the real length L of the trajectory. On the other hand, $\langle L\rangle = \sqrt{Dt}$ with $t = L/v_{\mathrm{F}}$. Therefore, $\langle L\rangle/L = l_{el}/\langle L\rangle$. In addition, we assume that the only temperature-dependent cause of inelastic scattering is inelastic electron-phonon collisions, with a corresponding mean free path $l_{inel} \sim l_{inel}^{e-ph} \sim T^3$.
As a result, the effective probability for coherent excitations to pass through the phase coherence region in elastic scattering can be written in the form

$$\begin{aligned} \tau_r &= \frac{l_{el}}{l_{inel}} \cdot \frac{l_{el}}{\langle L\rangle} = \beta T^{3.5}, \\ \beta &= l_{el}^{3/2}(\hbar v_{\mathrm{F}})^{-1/2}(l_{inel}^{*}T^{*3})^{-1}. \end{aligned} \tag{7}$$

In accordance with the Landauer concept, we find the relative contribution to the conductance G in the phase coherence region by calculating the proportion $F(m)$ of coherent trajectories (those that return to the reservoir after m reflections from the boundary, starting with the trajectory with $m = 1$) and their contribution to the current and summing over all trajectories:

$$\frac{\delta G}{G_0} = \sum_{m=1}^{\infty} F(m)I(m), \tag{8}$$

where $\delta G = G - G_0$, $G_0 \equiv G_{T=0}$; $F(m) = \tau_r^2(1-\tau_r)^{m-1}$ $(m \neq 0)$.
The probabilistic contribution to the current from a charge on trajectory with reflections is (Blonder et al., 1982; Van Wees et al., 1992)

$$I(m) = 1 + |r_{eh}(m)|^2|r_{ee}(m)|^2, \qquad |r_{eh}(m)|^2 + |r_{ee}(m)|^2 = 1,$$

where $|r_{ee}(m)|^2$ and $|r_{eh}(m)|^2$ are the probabilities for an electron incident on the *NS* boundary, to leave the boundary after m reflections in the form of an electron wave or a hole (Andreev) wave, respectively. The expression for $I(m)$ shows that for a large enough number of reflections, which increases the probability of Andreev reflection to such a degree that $|r_{eh}(m)|^2 \to 1$, the contribution of the corresponding trajectory to the current increases by a factor of 2. If all of those trajectories reached the reservoir, the dissipation would be increased by the same factor. Formally this is a consequence of the same fundamental conclusion of the theory which was mentioned above: in coherent Andreev reflection the efficiency of the elastic scattering of the electron momentum increases as a result of the interference of the e and h excitations. Actually, the fraction of the coherent trajectories that returns to the reservoir decreases rapidly with increasing distance to the reservoir from the boundary and with increasing number of reflections, which determines the length of the trajectory; thus we have the directly opposite result. In fact, assuming that for low electron energies $(eV/(\hbar v_{\mathrm{F}}/l_{el}) \ll 1)$ and a large contact area the main contribution to the change in

conductivity is from coherent trajectories with large numbers of reflections, so that $I(m) \approx 2$, and converting the sum in Eq. (8) to an integral, we find to a second approximation:

$$\frac{\delta G}{G_0} \approx 2\int_1^{m^*} F(m)dm \approx -\tau_r^2(m^{*2}\tau_r - 2m^*). \tag{9}$$

The upper limit of integration m^* is the number of reflections corresponding to a certain critical length for a coherent trajectory L that reaches the reservoir. This limit can be introduced as $m^* = \gamma\tau_r^{-1}$ with a certain coefficient γ that is to be determined experimentally. Substituting m^* into Eq. (9), we finally obtain

$$\frac{\delta G}{G_0} \approx -(\gamma^2 - 2\gamma)\tau_r = -AT^{3.5}, \qquad A = \beta(\gamma^2 - 2\gamma). \tag{10}$$

The nature of the effect consists in the fact that the number of trajectories leaving from the number of attainable reservoirs increases in the long-range phase coherence region, i.e., an ever greater number of trajectories appear on which the phase of the coherent wave functions does not relax; this decreases the dissipation. Thus, in accordance with Eq. (9), one expects that the temperature dependence of the relative effective resistance measured at the probes located within the phase coherence region will be in the form of a function that decreases with decreasing temperature below T_c as curve *1* in Fig. 3:

$$R/R_N = (R_0/R_N)(1 + AT^{3.5}). \tag{11}$$

2.1.2 Natural NS boundary

The discovery of an unusual increase in the resistance of normal conductors upon the appearance of an NS boundary (Figs. 1, 2) pointed to the need to deeper understand the properties of the systems with such boundaries. Since then study of the unconventional behavior of the electron transport in such systems has been taken on a broader scope.

As it was noted in Introduction, the early experiments detecting the phase-coherent contribution of quasiparticles to the kinetic properties of normal metals were carried out on samples that did not contain NS boundaries. In such a case this contribution, due solely to the mechanism of weak localization of electrons, appears as a small quantum interference correction to the diffusional contribution. Nevertheless, the existence of coherent transport under those conditions was proved experimentally. Study of the NS structures containing singly connected type I superconductors in the intermediate state, with large electron elastic mean free path, l_{el}, revealed resistance quantum oscillations of a type similar to the Aharonov-Bohm effect (Tsyan, 2000). The temperature - dependent resistances of Pb and In plates and Sn constriction were studied. The intermediate state was maintained by applying a weak external transverse magnetic field $\mathbf{B}_{ext}$ to the plates and by a self-current field $\mathbf{B}_I$ in the constriction. Thickness of Pb plates was 20 μm, with a separation $L_m \approx 250$ μm between the measuring probes in the middle part of the samples. A rolled In slab with dimensions $L \times W \times t = 1.5$ mm $\times$ 0.5 mm $\times$ 50 μm was soldered at its ends to one of the faces of a copper single crystal and was separated from this face by an insulating spacer. Measurements of the system with In were carried out at a direct current 0.7 A, which self-current magnetic field at a surface of the slab with the specified sizes made 5 G. The tin constriction was $t \approx 20$ μm in diameter and $L \approx 50$ μm in length, with $L_m \approx 100$ μm. At the constriction surface, B_I amounted to ≈ 100 G at $I = 1$ A. The bulk elastic mean free path in the

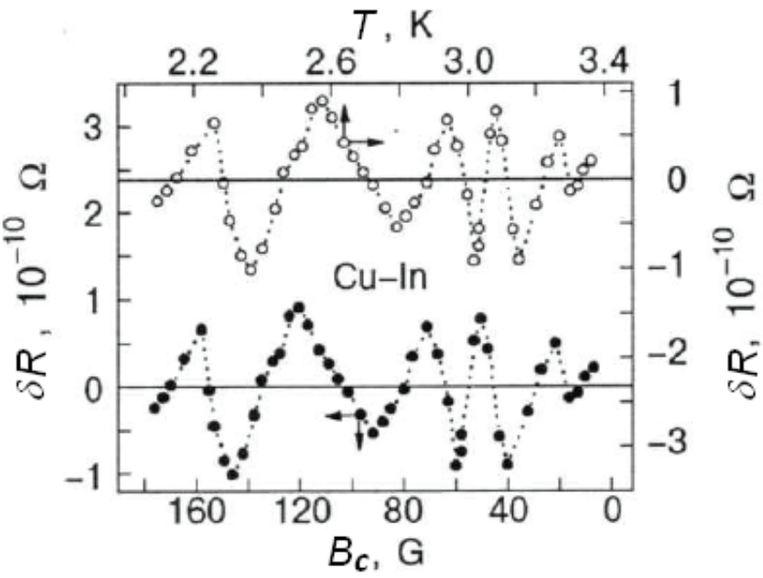


Fig. 6. R - oscillations for the doubly connected Cu-In system as a function of temperature (upper curve) and of the critical magnetic field (lower curve) at temperatures below T_c^{In} in the self-magnetic field (~ 5 G) of the measuring direct current.

workpieces from which the samples were fabricated was $l_{el} \sim 100$ μm. Such macroscopical value of elastic mean free path in macroscopical statement of experiment makes it necessary to measure samples of $(0.1 \div 1)\, l_{el}^3$ in volume, which resistance may make down to $10^{-8} \div 10^{-9}$ Ohm.

Figures 4, 5, and 6 show the oscillatory parts of the current-normalized potential difference δR (hereinafter referred to as R - oscillations), obtained by subtracting the corresponding mean monotonic part for each of the samples. It follows from these graphs that the resistances of the samples oscillate in temperature in the fields maintaining the intermediate state. As is seen, the oscillation amplitude $(\delta R)_{max}$ weakly depends on the temperature and the external magnetic field (although the monotonic resistance components vary over no less than two orders of magnitude). The character of oscillations in the Pb plate at various B_{ext} values (Fig. 4) indicates that the oscillation phase ϕ depends on the strength and sign of the external magnetic field: ϕ(480 G) is shifted from ϕ(550 G) by approximately π, while ϕ(520 G) and ϕ(550 G) coincide.

Constructing the critical-field scale for the oscillation region according to the equation $B_c(T) \simeq B_c(0)[1 - (T/T_c(0))^2]$ (T_c is the superconducting transition temperature), one finds that the oscillation period Δ_B in a magnetic field is constant for any pair of points one period apart and is equal to the difference in the absolute values of the critical field (see Figs. 4 and 5) for each of the samples. Here, we used $B_c^{\mathrm{Pb}}(0) = 803$ G and $B_c^{\mathrm{Sn}}(0) = 305$ G ((Handbook, 1974-1975)). This suggests that the $\Delta_B(B_c)$ period is a function of the direct rather than inverse field. The temperature T^* corresponding to the onset of R-oscillations in the Sn constriction is equal to the temperature for which $B_c^{\mathrm{Sn}}(T^*) = B_I(\approx 100$ G), viz., the temperature of the appearance of the intermediate state. The conditions for the confident resolution of the oscillations were fully satisfied for this sample up to 3.5 K. With the values of B_{ext} used for the Pb plate, T^* should lie outside the range of helium temperatures.

It is known that in the intermediate state of a type-I superconductor in a magnetic field, a laminar domain structure arises, with alternating normal and superconducting regions. The

observed dependence of the magnitude of the effect on the critical field in the intermediate state, first, provides direct evidence for the presence of a laminar domain NS structure and, second, indicates that the mechanism responsible for the R-oscillations occurs in the normal areas of domains, where, as is known, the magnetic field is equal to the superconductor critical field $B_c(T)$ (De Gennes, 1966). The use of the phenomenological theory of superconductivity (De Gennes, 1966; Lifshitz & Sharvin, 1951) for estimating the number of domains between the measuring probes brought about the values of approximately 12 at 3 K and 16 at 1.5 K for the Pb plate, 1 or 2 for the Sn constriction, and the value of 15-22 mm for the distance d_n between the NS boundaries in the oscillation region of interest. These data suggest the lack of any correlation between the indicated numbers and the number of observed oscillation periods.

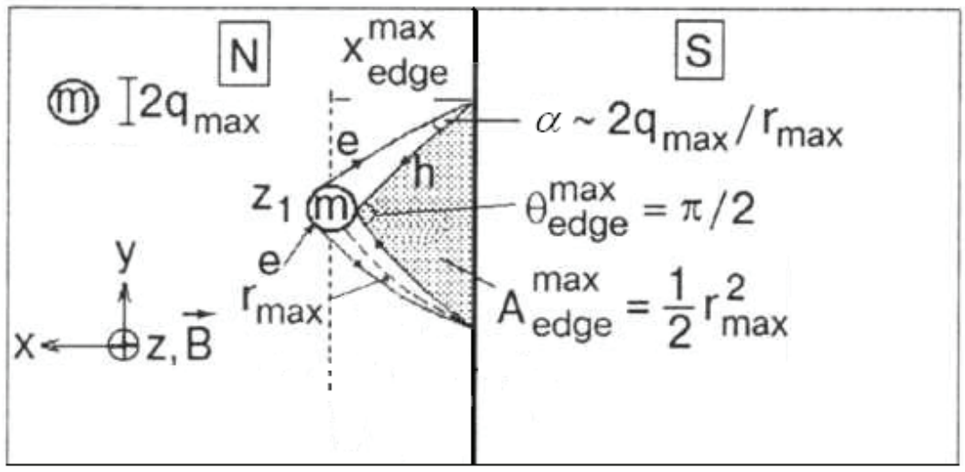


Fig. 7. The criterion of coherent interaction of an electron e and an Andreev hole h with the same elastic scattering center (see Eq. (12) in the text) establishes a distribution of areas A of quantization of the flux of the magnetic vector potential. The maximum admissible area $A^{\max}_{\text{edge}}$, bounded by the ballistic trajectories passing through the impurities m of maximum cross section $\sim q^2_{\max}$ at the positions $[x^{\max}_{\text{edge}},\ y,\ z]$ for $\theta^{\max}_{\text{edge}} = \pi/2$ is separated.

As is known, the direct dependence of the oscillation phase on the field strength arises when the quantization is associated with a real-space "geometric" factor, i. e., with the interference of coherent excitations on the geometrically specified closed dissipative trajectories in a magnetic vector-potential field (Aharonov & Bohm, 1959; Altshuler et al., 1981). At distances of the order of the thermal length $\xi_T \sim \xi_0 \approx \hbar v_{\text{F}}/k_{\text{B}}T$ from the NS boundary, where $l_{el} \gg \xi_0$, the main type of dissipative trajectories are those coherent trajectories on which the elastic-scattering center (impurity) interacts simultaneously with the coherent e (usual) and h (Andreev) excitations (Herath & Rainer, 1989; Kadigrobov, 1993). It was demonstrated in (Herath & Rainer, 1989) that, owing to the doubled probability for the h excitations to be scattered by the impurity, the interference on these trajectories generated the R-oscillations. In the presence of an electric field alone, neither the impurity nor the relevant coherent - trajectory size are set off, so that the oscillations do not arise (Kadigrobov et al., 1995; Van Wees et al., 1992).

Since the e and h trajectories spatially diverge in a magnetic field, the distance r from the impurity to the outermost boundary point, from which the particle can return to the same impurity after being Andreev-reflected, is bounded, according to the simple classical

geometric considerations, by the value

$$r = \sqrt{2qR_{\mathrm{L}}[B_c(T)]}. \tag{12}$$

In Eq. (12), R_{L} is the Larmor radius and q is the parameter (of the order of a screening radius) characterizing the impurity size. For instance, in fields of several hundred Gauss, $R_{\mathrm{L}} \approx 1.5 \cdot 10^{-2}$ cm and r does not exceed (1-2) μm at $q \approx (2-5) \cdot 10^{-8}$ cm; i. e., $\xi_0 \leq r \leq \xi_T \sim 10^{-2} l_{el}$ ($l_{el} \gg d_n$, ξ_T; $\xi_T \approx 3$ μm). Therefore, for every impurity with coordinate z, the magnetic field separates in the z = const plane a finite region of possible coherent trajectories passing through the impurity and closing two arbitrary reflection points on the NS boundary between the two most distant points which positions are determined by Eq. (12) (see Fig. 7). After averaging over all impurities, only a single trajectory (or a group of identical trajectories) specified by the edge of integration over the quantization area A makes an uncompensated contribution to the wave-function phase. The integration edge $A_{\mathrm{edge}} = (1/2)r_{\max}^2$ corresponds to the area bounded by the trajectory passing through the most efficient (with $\sim q_{\max}^2$) impurity situated at a maximum distance from the boundary, as allowed by criterion (12). One can easily verify that in our samples with $l_{el} \leq 0.1$ mm, every layer of impurity-size thickness parallel to the NS boundary comprises no less than 10^3 impurities; i. e., the coherent trajectories corresponding to the integration edge continuously resume upon shifting or the formation of new NS boundaries, so that A_{edge} is a continuously defined constant accurate to $\sim q_{\max}/r_{q_{\max}} \sim 10^{-4}$. According to (Aronov & Sharvin, 1987; Chiang & Shevchenko, 1999), the wave-function phase of the excitations with energy $E = eU$ in the field B should change along a coherent trajectory of length Λ as follows

$$\phi = \phi_e + \phi_h = 2\pi[(1/\pi)(E/\hbar v_{\mathrm{F}})\Lambda + BA/(\Phi_0/2)], \tag{13}$$

where $\Phi_0 = hc/e = 4.14 \cdot 10^{-7}$ G·cm^2. The first term in Eq. (13) can be ignored because, in our samples, it does not exceed 10^{-5} at $U \leq 10^{-8}$ V. One can thus expect that the interference contribution coming from the elastic-scattering centers to the conductivity oscillates as $\delta R \propto \delta R_{\max} \cos\phi$ (Chiang & Shevchenko, 2001), where $\delta R_{\max}$ is the amplitude depending on the concentration of the most efficient scattering centers and, hence, proportional to the total concentration c.

The maximum number of oscillation periods $\Delta B_{ext;I}$ that can be observed in a magnetic field upon changing the temperature clearly depends on the B_c variation scale. It varies from the value $B_c(T_O) = B_{ext;I}$ at the temperature T_O at which the SNS structure with the intermediate state arises, to the value $B_c(T)$ at a given temperature. Therefore, the phase of the oscillations at a given temperature should depend on the values of $B_{ext;I}$ in a following way:

$$\phi = 2\pi \frac{[B_c(T) - B_{ext;I}]A_{\max}}{\Phi_0/2}. \tag{14}$$

To estimate the interval of B_c values within which the change in A_{edge} with varying B_c may be neglected, we used Eq. (14) and the differential of the parameter r from Eq. (12). This yields $\Delta B_c \approx 3\Delta B_{ext;I}$.

From the condition $\Delta B \cdot A_{\mathrm{edge}} = \Phi_0/2$ and $\Delta B \approx (45;50)$ G, we obtain $r \approx 1$ μm, in accordance with the above-mentioned independent estimation. The ratio of the oscillation amplitudes also conforms to its expected value: $[(\delta R_{osc})^{\mathrm{Sn}}/(\delta R_{osc})^{\mathrm{Pb}}] \sim (c^{\mathrm{Sn}}/c^{\mathrm{Pb}}) \sim (l_{el}^{\mathrm{Pb}}/l_{el}^{\mathrm{Sn}}) \sim 10$. One can expect that a change in the number of domains in the plate from 12 to 16 alters the oscillation amplitude by no more than 40%; i. e., it only modifies the

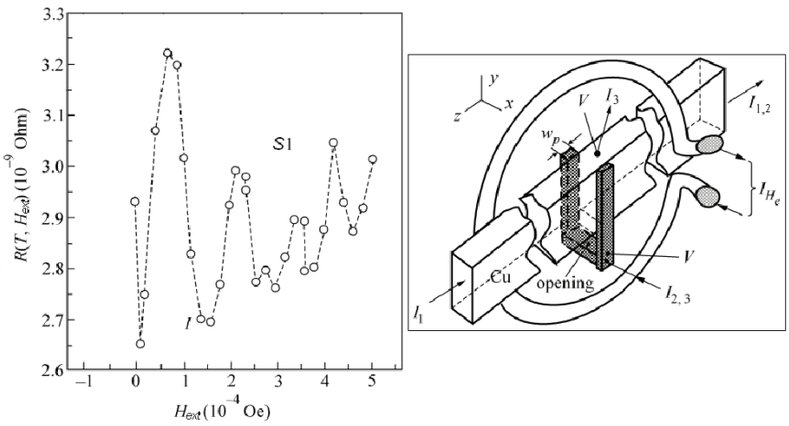


Fig. 8. Oscillations of the generalized resistance of the interferometer $s1$ (In-Cu-Sn) vs magnetic field at $T = 3.25$ K. The oscillation period is $\Delta H = (hc/2e)/A_{\max}$, where $A_{\max}$ is the area of the *abcd* contour in the (xy) cross section of the interferometer (see right panel).

oscillations but does not disturb the overall periodicity pattern (Fig. 4). It also follows from Eq. (14) that the number of periods between the temperature of oscillation onset, $T_{\rm O}$, and an arbitrary temperature depends on the value of $B_c(T_{\rm O}) = B_{ext}$. This makes understandable the relation between the phases of oscillations observed for the Pb plate in different fields: $(\phi_{550G} - \phi_{480G}) \approx 3\pi$ and $(\phi_{520G} - \phi_{480G} + \pi) \approx 3\pi$ (it is taken into account that **B**[520 G] = -**B**[480 G]). Such a relation is a result of the different number of periods, ΔB, measured from $B_{ext;I}$.

The significant distortions of the shape of the oscillation curves in the Pb sample is most likely due to variations in the value of $q_{\max}$ when the number of domains varies in the investigated temperature interval, thereby changing the position of the NS boundaries.

In the sample containing In, the values of $T_{\rm O}$ and $T_c(B = 0)$ are extremely close to each other because of the small $B_I \approx 5$ G. As a result, in the same temperature interval as for Sn and Pb one can observe more than three oscillation periods (compare Figs. 5 and 6). In such case, the change in $A_{\max}$ and, hence, in the oscillation period is hardly noticeable (see the estimation above).

It is appropriate here to compare (although qualitatively) the order of magnitude of the interference contributions to the conductance in the absence of an NS boundary, in the approximation of a weak-localization mechanism, and in the presence of an NS boundary. According to the theory of weak localization (Altshuler et al., 1980), the probability of an occurrence of self-intersecting trajectories is of the order of $(\lambda_{\rm B}/l_{el})^2 \sim 10^{-7}$ ($\lambda_{\rm B}(\sim q)$ is the de Broglie wavelength; $l_{el} \approx 100$ μm), while as the probability that coherent trajectories will arise in the case of an NS boundary in a layer with a characteristic size of the order of the mean free path is larger by a factor of $(r/\lambda_{\rm B})^2 \sim 10^8$ than the probability of formation of self-crossing trajectories. The existence of coherent trajectories in the NS system is determined by the area of the base of the cone formed by accessible coherent trajectories arising as a result of Andreev reflection, the base of the cone resting on the superconductor and the vertex at an impurity (see Fig. 7). Hence, the expected relative interference contribution to the resistance of an NS system is as follows

$$(\delta R/R) \sim (r/\lambda_{\rm B})^2(\lambda_{\rm B}/l_{el})^2 \gg 1, \tag{15}$$

and agrees completely with the amplitude of the oscillations we observed in a Pb slab.

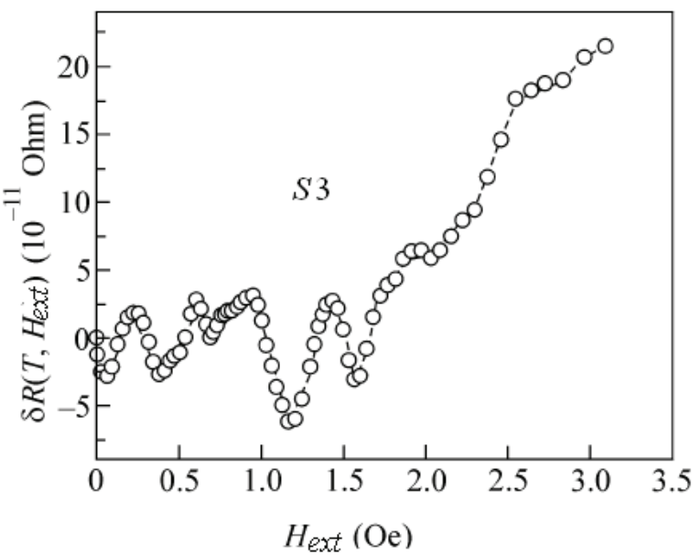


Fig. 9. Oscillations of "Andreev resistance" $\delta R = R(H_{ext}) - R(H_{ext} = 0)$ in interferometer $s3$ (Pb/Cu/Pb) as a function of magnetic field at $T = 4.125$ K. The oscillation period is $\Delta H = (hc/2e)/A_{min}$, where A_{min} is the area of xy projection of the stretched opening of the interferometer onto the direction of magnetic field upon the deviation from the z axis; $R(H_{ext} = 0) = 2.6245 \times 10^{-8}$ Ohm.

2.2 Doubly connected SNS structures

Below we present the results from the study of the conductance of doubly connected NS systems. Similarly to singly connected ones considered above, they meet the same "macroscopic" conditions, namely, L, $l_{el} \gg \xi_T = \xi_0$ $(L/\xi_T \approx 100)$. This means that a spatial scale of the possible proximity effect is much less than the size of a normal segment of the system, this effect can be therefore neglected completely when considering phenomena of the interferential nature in such "macroscopical" systems.

Macroscopical hybrid samples $s1$ [In(S)/Cu(N)/Sn(S)], $s2$ [Sn(S)/Cu(N)/Sn(S)], $s3$ [Pb(S)/Cu(N)/Pb(S)], and [In(S)/Al(N)/In(S)] were prepared using a geometry of a doubly connected SNS Andreev interferometer with a calibrated opening. Figures 8 (right panel) and 10 (upper panel) show schematically (not to scale) the typical construction of the samples, together with a wire turn as a source of an external magnetic field $H_{\rm ext}$ for controlling the macroscopic phase difference in the interferometer formed by a part of a normal single crystal (Cu, Al) and a superconductor connected to it. Interferometers varied in size, type of a superconductor, and area of the NS interfaces. The field $H_{\rm ext}$ was varied within a few Oersteds in increments of 10^{-5} Oe. An error of field measurement amounted to no more than 10 %. To compensate external fields, including the Earth field, the container with the sample and the turn was placed into a closed superconducting shield.

Conductance of all the systems studied oscillated while changing the external magnetic field which was inclined to the plane of the opening. It has thus appeared that the areas of extreme projections, S_{extr}, onto the plane normal to the vector of the external magnetic field are related to the periods of observed oscillations, ΔH, by the expression $S_{extr}\Delta H = \Phi_0$, where Φ_0 is the magnetic flux quantum $hc/2e$. The values of $S_{\rm min}$ and $S_{\rm max}$ differed from each other by more than an order of magnitude for each of the interferometers, allowing the corresponding oscillation periods to be resolved (see Figs. 8 - 10).

The sensitivity of dissipative conduction to the macroscopic phase difference in a closed SNS contour is a direct evidence for the realization of coherent transport in the system and the role played by both NS interfaces in it. In turn, at $L \gg \xi_T$, the coherent transport can be caused by only those normal-metal excitations which energies, $\varepsilon \ll T < \Delta$, fill the Andreev spectrum that arises due to the restrictions on the quasiparticle motion because of the Andreev reflections (Zhou et al., 1995). It follows from the quasiclassical dimensional quantization (Andreev, 1964; Kulik, 1969) that the spacing between the levels of the Andreev spectrum should be $\varepsilon_{\rm A} \approx \hbar v_{\rm F}/L_x \approx 20$ mK for the distance between NS interfaces $L_x \simeq$ 0.5 mm. It corresponds to the upper limit for energies of the $e-h$ excitations on the dissipative (passing through the elastic scattering centers) coherent trajectories in the normal region. To zero order in the parameter $\lambda_{\rm B}/l$, only these trajectories can make a nonaveraged phase-interference contribution to conductance, often called the "Andreev" conductance $G_{\rm A}$ (Lambert & Raimondi, 1998). Accordingly, it was supposed that the modulation depth for the normal conductance G_N (or resistance R_N) in our interferometers in the temperature range measured would take the form

$$1 - \frac{G_{\rm A}}{G_N} \equiv \frac{\delta R_{\rm A}}{R_N} \approx \frac{\varepsilon_{\rm A}}{T} \simeq 10^{-2}. \tag{16}$$

In the approximation of noninteracting trajectories, the macroscopic phase, ϕ_i, which coherent excitations with phases ϕ_{ei} and ϕ_{hi} is gaining while moving along an i-th trajectory closed by a superconductor, depends in an external vector-potential field $\mathbf{A}$ on the magnetic flux as follows

$$\phi_i = \phi_{ei} + \phi_{hi} = \phi_{0i} + 2\pi\frac{\Phi_i}{\Phi_0}, \tag{17}$$

where ϕ_{0i} is the microscopic phase related to the length of a trajectory between the interfaces by the Andreev-reflection phase shifts; $\Phi_i = \mathbf{H}_{ext} \cdot \mathbf{S}_i$ is the magnetic flux through the projection S_i onto the plane perpendicular to $\mathbf{H}_{ext}$; $\mathbf{H}_{ext} = \nabla \times \mathbf{A}$ is the magnetic field vector; $\mathbf{S}_i = \mathbf{n}_{S_i} \cdot S_i$; $\mathbf{n}_{S_i}$ is the unit normal vector; S_i is the area under the trajectory; and Φ_0 is the flux quantum $hc/2e$.

The evaluation of the overall interference correction, $2{\rm Re}(f_e f_h^*)$, in the expression for the total transmission probability $|f_e + f_h|^2$ ($f_{e,h}$ are the scattering amplitudes) along all coherent trajectories can be reduced to the evaluation of the Fresnel-type integral over the parameter $\mathbf{S}_i$ (Tsyan, 2000). This results in the separation of the $\mathbf{S}$-nonaveraged phase contributions at the integration limits. As a result, the oscillating portion of the interference addition to the total resistance of the normal region in the SNS interferometer, in particular, for $\mathbf{H}_{ext}||z$, takes the form

$$\frac{\delta R_{\rm A}}{R_N} \sim \frac{\varepsilon_{\rm A}}{T}\sin[2\pi(\phi_0 + \frac{H_{ext}S_{extr}}{\Phi_0})], \tag{18}$$

where S_{extr} is the minimal or maximal area of the projection of doubly connected SNS contours of the system onto the plane perpendicular to $\mathbf{H}$, and $\phi_0 \sim (1/\pi)(L/l_{el}) \sim 1$ (Van Wees et al., 1992). Our experimental data are in good agreement with this phase dependence of the generalized interferometer resistance and the magnitude of the effect. Since all doubly connected SNS contours include $e-h$ coherent trajectories in the normal region with a length of no less than $\sim L \approx 10^2\xi_T$, one can assert that the observed oscillations are due to the long-range quantum coherence of quasiparticle excitations under conditions of suppressed proximity effect for the major portion of electrons.

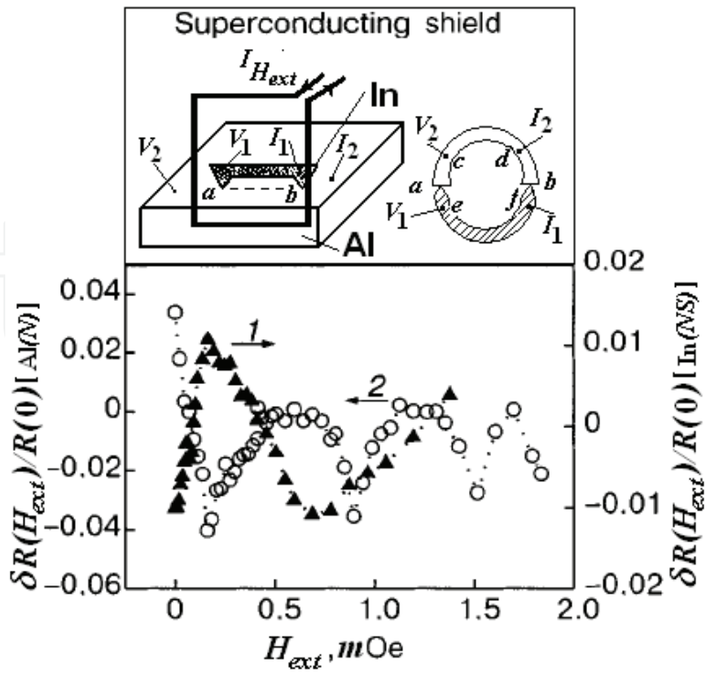


Fig. 10. Non-resonance oscillations of the phase-sensitive dissipative component of the resistance of the indium narrowing (curve *1*) at $T = 3.2$ K and the resonance oscillations of this component in the aluminum part (curve *2*) at $T = 2$ K for the interferometer with $R_a \ll R_b$, as functions of the external magnetic field.

3. Macroscopical NS systems with a magnetic N - segment

The peculiarities of electron transport arising due to the influence of a superconductor contacted to a normal metal and, particularly, to a ferromagnet (F) have been never deprived of attention. Recently, a special interest in the effects of that kind has been shown, in connection with the revived interest to the problem of nonlocal coherence (Hofstetter et al., 2009). Below we demonstrate that studying the coherent phenomena associated with the Andreev reflection, in the macroscopical statement of experiments, may be directly related to this problem. As is known, even in mesoscopic NS systems, the coherent effects has been noted in a normal-metal (magnetic) segment at a distance of $x \gg \xi_{\text{exch}}$ from a superconductor (ξ_{exch} is the coherence length in the exchange field of a magnetic) (Giroud et al., 2003; Gueron et al., 1996; Petrashov et al., 1999). That fact gave rise to the intriguing suggestion that magnetics could exhibit a long-range proximity effect, which presumed the existence of a nonzero order parameter $\Delta(x)$ at the specified distance. Such a suggestion, however, contradicts the theory of FS junctions, since $\xi_{\text{exch}} \ll \xi_T \sim v_{\text{F}}/T$, and v_{F}/T is the ordinary scale of the proximity effect in the semiclassical theory of superconductivity (De Gennes, 1966). This assumption, apparently, is beneath criticism, because of the specific geometry of the contacts in mesoscopic samples. As a rule, these contacts are made by a deposition technology. Consequently, they are planar and have the resistance comparable in value with the resistance of a metal located under the interface. A shunting effect arises, and the estimation of the value and even sign of the investigated transport effects becomes ambiguous (Belzig et al., 2000; Jin & Ketterson, 1989; De Jong & Beenakker, 1995).

Influence of the shunting effect is well illustrated by our previous results (Chiang & Shevchenko, 1999); one of them is shown in Fig. 11. The conductance measured outside the *NS* interface (see curve *1* and Inset 1) behaves in accordance with the fundamental ideas of the semiclassical theory (see Sec. 2. 1): Because of "retroscattering", the cross section for elastic scattering by impurities in a metal increases at the coherence length of $e-h$ hybrids formed in the process of Andreev reflection, i. e., the conductivity of the metal decreases rather than increases. Additional scattering of Andreev hole on the impurity is completely ignored in case of a point-like ballistic junction (Blonder et al., 1982). At the same time, the behavior of the resistance of the circuit which includes a planar interface (see Inset 2) may not even reflect that of the metal itself (curve *2*; see also (Petrashov et al., 1999)), but it is precisely this type of behavior that can be taken as a manifestation of the long-range proximity effect.

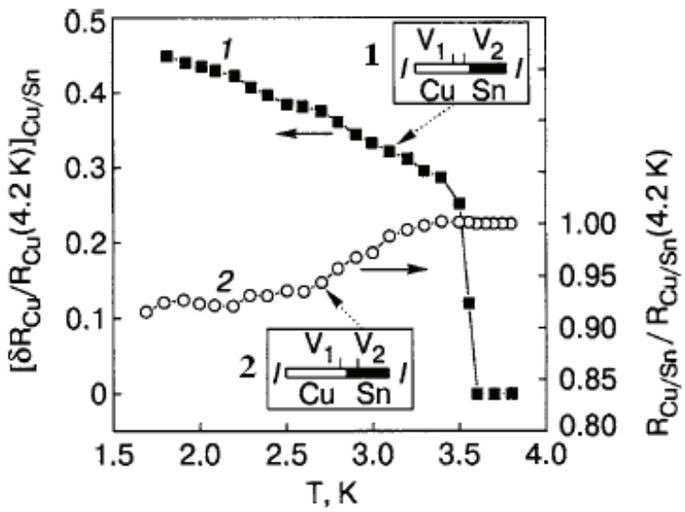


Fig. 11. Temperature dependences of the resistance of the system normal metal/superconductor in two measurement configurations: outside the interface (curve *1*, Inset 1) and including the interface (curve *2*, Inset 2).

3.1 Singly connected *FS* systems

Here, we present the results of experimental investigation of the transport properties of non-film single - crystal ferromagnets Fe and Ni in the presence of *F*/ In interfaces of various sizes (Chiang et al., 2007). We selected the metals with comparable densities of states in the spin subbands; conducting and geometric parameters of the interfaces, as well as the thickness of a metal under the interface were chosen to be large in comparison with the thickness of the layer of a superconductor. In making such a choice, we intended to minimize the effects of increasing the conductivity of the system that could be misinterpreted as a manifestation of the proximity effect.

The geometry of the samples is shown (not to scale) in Fig. 12. The test region of the samples with *F*/*S* interfaces *a* and *b* is marked by a dashed line. After setting the indium jumper, the region *abdc* acquired the geometry of a closed "Andreev interferometer", which made it possible to study simultaneously the phase-sensitive effects. Both point (*p*) and wide (*w*) interfaces were investigated. We classify the interface as "point" or "wide" depending on the ratio of its characteristic area to the width of the adjacent conductor (of the order of 0.1 or 1, respectively).

3.1.1 Doubling the cross section of scattering by impurities

Figure 13 shows in relative units $\delta R/R = [R(T) - R(T = T_c^{\rm In})]/R(T = T_c^{\rm In})$ the resistance of the ferromagnetic segments with point (Fe, curve *1* and Ni, curve *2*) and wide (Ni, curve *3*) F/S interfaces measured with current flow *parallel* to the interfaces [for geometry, see Insets (a) and (b)]. In this configuration, with indium in the superconducting state, the interfaces, as parts of the potential probes, play a passive role of "superconducting mirrors". It can be seen that for $T \leq T_c^{\rm In}$ (after Andreev reflection is actuated), the resistance of Ni increases abruptly by 0.04% ($\delta R_p \approx 1 \times 10^{-8}$ Ohm) in the case of two point interfaces and by 3% ($\delta R_w \approx 7 \times 10^{-7}$ Ohm) in the case of two wide ones. In Fe with point interfaces, a negligible effect of opposite sign is observed, its magnitude being comparable to that in Ni, $\delta R_p^{\rm Ni}$.
Just as in the case of a nonmagnetic metal (Fig. 11), the observed decrease in the conductivity of nickel when the potential probes pass into the "superconducting mirrors" state, corresponds to an increase in the efficiency of the elastic scattering by impurities in the metal adjoining the superconductor when Andreev reflection appears. (We recall that the shunting effect is small). In accordance with Eq. (3), the interference contribution from the scattering of a singlet pair of $e-h$ excitations by impurities in the layer, of the order of the coherence length ξ in thickness, if measured at a distance L from the N/S interface, is proportional to ξ/L. From this expression one can conclude that the ratio of the magnitude of the effect, δR, to the resistance measured at an arbitrary distance from the boundary is simply the ratio of the corresponding spatial scales. It is thereby assumed that the conductivity σ is a common parameter for the entire length, L, of the conductor, including the scale ξ. Actually, we find from Eq. (3) that the magnitude of the positive change in the resistance, δR, of the layer ξ in whole is

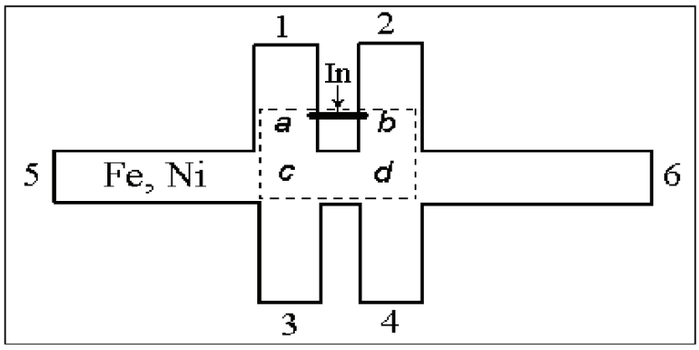


Fig. 12. Schematic view of the F/S samples. The dashed line encloses the workspace. F/In interfaces are located at the positions a and b. The regimes of current flow, parallel or perpendicular to the interfaces, were realized by passing the feed current through the branches 1 and 2 with disconnected indium jumper $a-b$ or through 5 and 6 when the jumper was closed (shown in the figure).

$$\delta R^{\,\xi} = (\xi/\sigma_\xi A_{\rm if})\bar{r} \equiv \sum_{i=1}^{N_{\rm imp}} \delta R_i^{\,\xi}. \tag{19}$$

Here, σ_ξ is the conductivity in the layer ξ; $A_{\rm if}$ is the area of the interface; $N_{\rm imp}$ is the number of Andreev channels (impurities) participating in the scattering; δR_i^{ξ} is the resistance resulting from the $e-h$ scattering by a single impurity, and $\bar{r}$ is the effective probability for elastic scattering of excitations with the Andreev component in the layer ξ as a whole. Control

measurements of the voltages in the configurations included and not included interfaces showed that in our systems, the voltages themselves across the interfaces were negligibly small, so that we can assume $\bar{r} \approx 1$. It is evident that the Eq. (19) describes the resistance of the ξ-part of the conductor provided that $\sigma_\xi = \sigma_L$ i. e., for $\xi > l_{el}$. For ferromagnets, $\xi \ll l_{el}$ and $l_{el}^L \neq l_{el}$. In this case, to compare the values of δR measured on the length L with the theory, one should renormalize the value of R_N from the Eq. (3).

In the semiclassical representation, the coherence of an Andreev pair of excitations in a metal is destroyed when the displacement of their trajectories relative to each other reaches a value of the order of the trajectory thickness, i. e., the de Broglie wavelength λ_B. The maximum possible distance ξ_m (collisionless coherence length) at which this could occur in a ferromagnet with nearly rectilinear e and h trajectories (Fig. 14a) is

$$\xi_m \sim \frac{\lambda_\mathrm{B}}{\varepsilon_{exch}/\varepsilon_F} = \frac{\pi\hbar v_\mathrm{F}}{\varepsilon_{exch}}; \qquad \varepsilon_{exch} = \mu_\mathrm{B} H_{exch} \sim T_{exch} \tag{20}$$

(μ_B is the Bohr magneton, H_{exch} is the exchange field, and T_{exch} is the Curie temperature). However, taking into account the Larmor curvature of the e and h trajectories in the field H_{exch}, together with the requirement that both types of excitations interact with the same impurity (see Fig. 14b), we find that the coherence length decreases to the value (De Gennes, 1966) $\xi^* = \sqrt{2qr} = \sqrt{2q\xi_m}$ (compare with Eq. (12)). Here, r is the Larmor radius in the field H_{exch} and q is the screening radius of the impurity $\sim \lambda_\mathrm{B}$. Figure 14 gives a qualitative idea of the scales on which the dissipative contribution of Andreev hybrids can appear, as a result of scattering by impurities ($N_\mathrm{imp} \gg 1$), with the characteristic dimensions of the interfaces $y, z \gg l_{el}$.

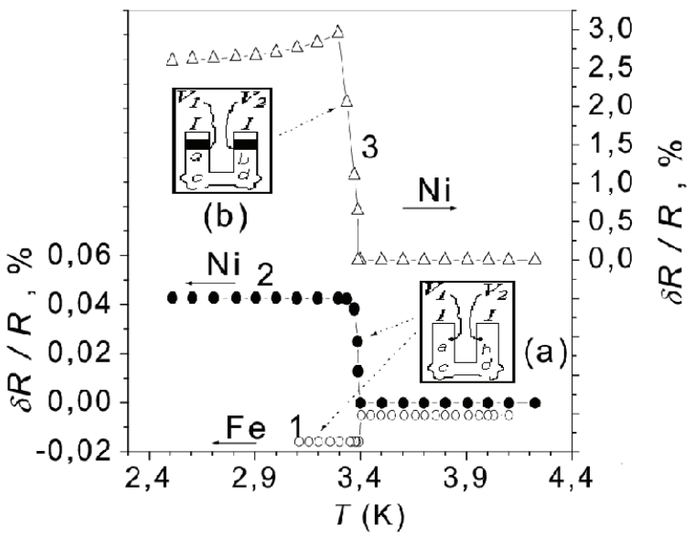


Fig. 13. Temperature dependences of the resistance of Fe and Ni samples in the presence of F/In interfaces acting as "superconducting mirrors" at $T < T_c^{\mathrm{In}}$. Curves *1* and *2*: Fe and Ni with point interfaces, respectively; curve *3*: Ni with wide interfaces. Insets: geometry of point (a) and wide (b) interfaces.

For Fe with $T_{exch} \approx 10^3$ K and Ni with $T_{exch} \approx 600$ K, we have $\xi^* \approx 0.001$ μm. It follows that in our experiment with $l_{el} \approx 0.01$ μm (Fe) and $l_{el} \approx 1$ μm (Ni), the limiting case $l_{el} \gg \xi^*$ and $l_{el}^L \neq l_{el}^{\tilde{\xi}}$ is realized. From Fig. 14b it can be seen that for $y, z \gg l_{el} \gg \xi^*$ in the normal

state of the interface, the length l_{el}^{ξ} within the layer ξ^* corresponds to the shortest distance between the impurity and the interface, i. e., $l_{el}^{\xi} \equiv \xi^*$ $(\sigma_L \neq \sigma_{\xi^*})$. Note that for an equally probable distribution of the impurities, the probability of finding an impurity at any distance from the interface in a finite volume, with at least one dimension greater than l_{el}, is equal to unity. Renormalizing Eq. (3), with ξ_T replaced by ξ^*, we obtain the expression for estimating the coherence correction to the resistance measured on the length L in the ferromagnets:

$$\frac{\delta R^{\xi^*}}{R_L} = \frac{\xi^*}{L} \cdot \frac{l_{el}}{l_{el}^{\xi^*}} \bar{r} \approx \frac{l_{el}}{L} \bar{r};\ \delta R^{\xi^*} = \frac{\xi^*}{\sigma_{\xi^* A_{if}}} \bar{r} \equiv \sum_{i=1}^{N_{imp}} \delta R_i^{\xi^*}. \tag{21}$$

Here, σ_{ξ^*} is the conductivity in the layer ξ^*; $\delta R_i^{\xi^*}$ is the result of $e-h$ scattering by a single impurity. Equation (21) can serve as an observability criterion for the coherence effect in ferromagnets of different purity. It explains why no positive jump of the resistance is seen on curve *1*, Fig. 13, in case of a point Fe/In interface: with $l_{el}^{\mathrm{Fe}} \approx 0.01$ μm, the interference increase in the resistance of the Fe segment with the length studied should be $\approx 10^{-9}$ Ohm and could not be observed at the current $I_{acdb} \leq 0.1$ A, at which the measurement was performed, against the background due to the shunting effect.

Comparing the effects in Ni for the interfaces of different areas also shows that the observed jumps pertain precisely to the coherent effect of the type studied. Since the number of Andreev channels is proportional to the area of an N/S interface, the following relation should be met between the values of resistance measured for the samples that differ only in the area of the interface: $\delta R_w^{\xi^*} / \delta R_p^{\xi^*} = N_{\mathrm{imp}}^w / N_{\mathrm{imp}}^p \sim A_w / A_p$ (the indices p and w refer to point and wide interfaces, respectively). Comparing the jumps on the curves *2* and *3* in Fig. 13 we obtain: $\delta R_w / \delta R_p = 70$, which corresponds reasonably well to the estimated ratio $A_w / A_p = 25 - 100$.

In summary, the magnitude and special features of the effects observed in the resistance of magnetics Fe and Ni are undoubtedly directly related with the above-discussed coherent effect, thereby proving that, in principle, it can manifest itself in ferromagnets and be observed provided *an appropriate instrumental resolution*. Although this effect for magnetics is somewhat surprising, it remains, as proved above, within the bounds of our ideas about the scale of the coherence length of Andreev excitations in metals, which determines the dissipation; therefore, this effect cannot be regarded as a manifestation of the proximity effect in ferromagnets.

3.1.2 Spin accumulation effect

The macroscopic thickness of ferromagnets under F/S interfaces made it possible to investigate the resistive contribution from the interfaces, R_{if}, in the conditions of current flowing perpendicular to them, through an indium jumper with current fed through the contacts 5 and 6 (see Fig. 12 and Inset in Fig. 15).

Figure 15 presents in relative units the temperature behavior of R_{if}^p for point Fe/In interfaces (curve *1*) and R_{if}^w for wide Ni/In interfaces (curve *2*) as $\delta R_{if}/R_{if} = [R_{if}(T) - R_{if}(T_c^{In})]/R_{if}(T_c^{In})$. The shape of the curves shows that with the transition of the interfaces from the F/N state to the F/S state the resistance of the interfaces abruptly *increases* but compared with the increase due to the previously examined coherent effect it increases by an incomparably larger amount. It is also evident that irrespective of the interfacial geometry the behavior of the function $R_{if}(T)$ is qualitatively similar in both systems. The value of $R_{if}(T_c^{In})$ is the lowest resistance of the interface that is attained when the current is displaced

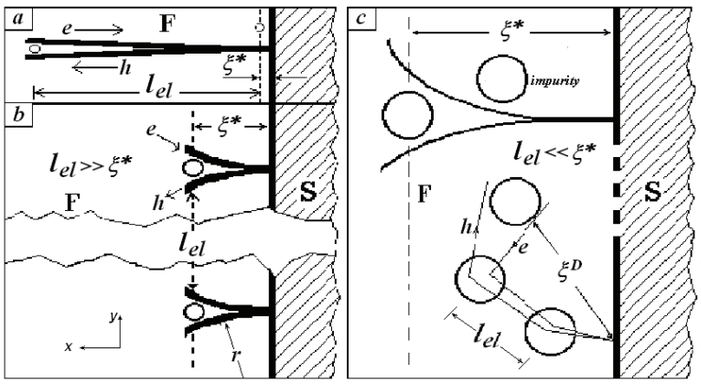


Fig. 14. Scattering of Andreev $e-h$ hybrids and their coherence length ξ^* in a normal ferromagnetic metal with characteristic F/S interfacial dimensions greater than l_{el}. Panels $a, b:\ \xi^* \ll l_{el}$; panel $c:\ \xi^* \gg l_{el};\ \xi^D \sim \sqrt{l_{el}\xi^*}$.

to the edge of the interface due to the Meissner effect. The magnitudes of the positive jumps with respect to this resistance, $\delta R_{if}/R_{if}(T_c^{In}) \equiv \delta R_{F/S}/R_{F/N}$, are about 20% for Fe (curve *1*) and about 40% for Ni (curve *2*). The values obtained are more than an order of

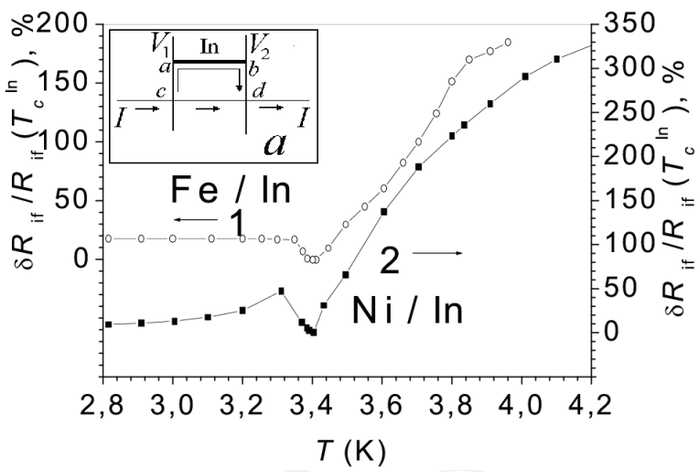


Fig. 15. Spin accumulation effect. Relative temperature dependences of the resistive contribution of spin-polarized regions of Fe and Ni near the interfaces with small (Fe/In) and large (Ni/In) area.

magnitude greater than the contribution to the increase in the resistance of ferromagnets which is related with the coherent interaction of the Andreev excitations with impurities (as is shown below, because of the incomparableness of the spatial scales on which they are manifested). This makes it possible to consider the indicated results as being a direct manifestation of the mismatch of the spin states in the ferromagnet and superconductor, resulting in the accumulation of spin on the F/S interfaces, which decreases the conductivity of the system as a whole. We suppose that such a decrease is equivalent to a decrease in the conductivity of a certain region of the ferromagnet under the interface, if the exchange spin splitting in the ferromagnetic sample extends over a scale not too small compared to the size of this region. In other words, the manifestation of the effect in itself already indicates that the dimensions of the region of the ferromagnet which make the effect observable are

comparable to the spin relaxation length. Therefore, the effect which we observed should reflect a resistive contribution from the regions of ferromagnets on precisely the same scale. The presence of such nonequilibrium regions and the possibility of observing their resistive contributions using a four-contact measurement scheme are due to the "non-point-like nature" of the potential probes (finiteness of their transverse dimensions). In addition, the data show that the dimensions of such regions near Fe/S and Ni/S interfaces are comparable in our experiments. Indeed, the value of $\delta R_{\mathrm{Ni}/S}/R_{\mathrm{Ni}/N}$ corresponding according to the configuration to the contribution from only the nonequilibrium regions and the value of $\delta R_{\mathrm{Fe}/S}/R_{\mathrm{Fe}/N}$ obtained from a configuration which includes a ferromagnetic conductor of length obviously greater than the spin-relaxation length, are actually of the same order of magnitude. In addition, according to the spin-accumulation theory (Hofstetter et al., 2009; Lifshitz & Sharvin, 1951; Van Wees et al., 1992), the expected magnitude of the change in the resistance of the F/S interface in this case is of the order of

$$\delta R_{F/S} = \frac{\lambda_s}{\sigma A} \cdot \frac{P^2}{1-P^2}; \qquad P = (\sigma_\uparrow - \sigma_\downarrow)/\sigma; \qquad \sigma = \sigma_\uparrow + \sigma_\downarrow. \tag{22}$$

Here, λ_s is the spin relaxation length; P is the coefficient of spin polarization of the conductivity; σ, $\sigma_\uparrow$, $\sigma_\downarrow$, and A are the total and spin-dependent conductivities and the cross section of the ferromagnetic conductor, respectively. Using this expression, substituting the data for the geometric parameters of the samples, and assuming $P^{\mathrm{Fe}} \sim P^{\mathrm{Ni}}$, we obtain $\lambda_s(\mathrm{Fe}/S)/\lambda_s^*(\mathrm{Ni}/S) \approx 2$. This is an additional confirmation of the comparability of the scales of the spin-flip lengths λ_s for Fe/S and λ_s^* for Ni/S, indicating that the size of the nonequilibrium region determining the magnitude of the observed effects for those interfaces is no greater than (and in Fe equal to) the spin relaxation length in each metal. In this case, according to Eq. (22), the length of the conductors, with normal resistance of which the values of $\delta R_{F/S}$ must be compared, should be set equal to precisely the value of λ_s for Fe/S and λ_s^* for Ni/S. This implies the following estimate of the coefficients of spin polarization of the conductivity for each metal:

$$P = \sqrt{(\delta R_{F/S}/R_{F/N})/[1 + (\delta R_{F/S}/R_{F/N})]}. \tag{23}$$

Using our data we obtain $P^{\mathrm{Fe}} \approx 45\%$ for Fe and $P^{\mathrm{Ni}} \approx 50\%$ for Ni, which is essentially the same as the values obtained from other sources (Soulen et al., 1998). If in Eq. (22) we assume that the area of the conductor, A, is of the order of the area of the current entrance into the jumper (which is, in turn, the product of the length of the contour of the interface by the width of the Meissner layer), then a rough estimate of the spin relaxation lengths in the metals investigated, in accordance with the assumption of single-domain magnetization of the samples, will give the values $\lambda_s^{\mathrm{Fe}} \sim 90$ nm and $\lambda_s^{\mathrm{Ni}} > 50$ nm. Comparing these values with the value of coherence length in ferromagnets $\xi^* \approx 1$ nm we see that although the coherent effect leads to an almost 100% increase in the resistance, this effect is localized within a layer which thickness is two orders of magnitude less than that of the layer responsible for the appearance of the spin accumulation effect, therefore it does not mask the latter.

3.2 Doubly connected SFS systems

The observation of the coherent effect in the singly connected FS systems raised the following question: Can effects sensitive to the phase of the order parameter in a superconductor be manifested in the conductance of ferromagnetic conductors of macroscopic size? To answer

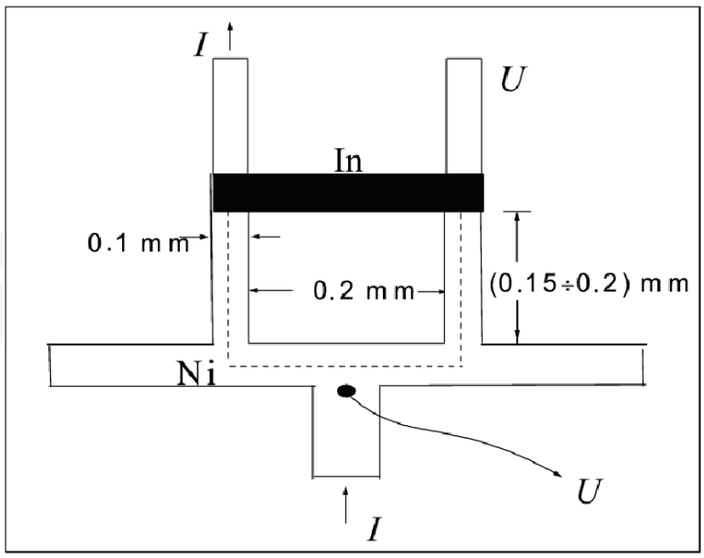


Fig. 16. Schematic diagram of the F/S system in the geometry of a doubly connected "Andreev interferometer". The ends of the single-crystal ferromagnetic (Ni) segment (dashed line) are closed by a superconducting In bridge.

this question we carried out direct measurements of the conductance of Ni conductors in a doubly connected SFS configuration (in the Andreev interferometer (AI) geometry shown in Fig. 16).

Figures 17 and 18 show the magnetic-field oscillations of the resistance of two samples in a doubly connected S/Ni/S configuration with different aperture areas, measured for the arrangement of the current and potential leads illustrated in Fig. 16. The oscillations in Fig. 17 are presented on both an absolute scale ($\delta R_{\rm osc} = R_H - R_0$, left axis) and a relative scale ($\delta R_{\rm osc}/R_0$, right axis). R_0 is the value of the resistance in zero field of the ferromagnetic segment connecting the interfaces in the area of a dashed line in Fig. 16. Such oscillations in SFS systems in which the total length of the ferromagnetic segment reaches the values of the order of 1 mm (along the dashed line in Fig. 16), were observed for the first time. Figures 17 and 18 were taken from two samples during two independent measurements, for opposite directions of the field, with different steps in H and are typical of several measurements, which fact confirms the reproducibility of the oscillation period and its dependence on the aperture area of the interferometer.

The period of the resistive oscillations shown in Fig. 17 is $\Delta B \approx (5-7) \times 10^{-4}$ G and is observed in the sample with the geometrical parameters shown in Fig. 16. It follows from this figure that the interferometer aperture area, enclosed by the midline of the segments and the bridge, amounts to $A \approx 3 \times 10^{-4}$cm^2. In the sample with twice the length of the sides of the interferometer and, hence, approximately twice the aperture area, the period of the oscillations turned out to be approximately half as large (solid line in Fig. 18). From the values of the periods of the observed oscillations it follows that, to an accuracy of 20%, the periods are proportional to a quantum of magnetic flux $\Phi_0 = hc/2e$ passing through the corresponding area A : $\Delta B \approx \Phi_0/A$.

Obviously, the oscillatory behavior of the conductance is possible if the phases of the electron wave functions are sensitive to the phase difference of the order parameter in the

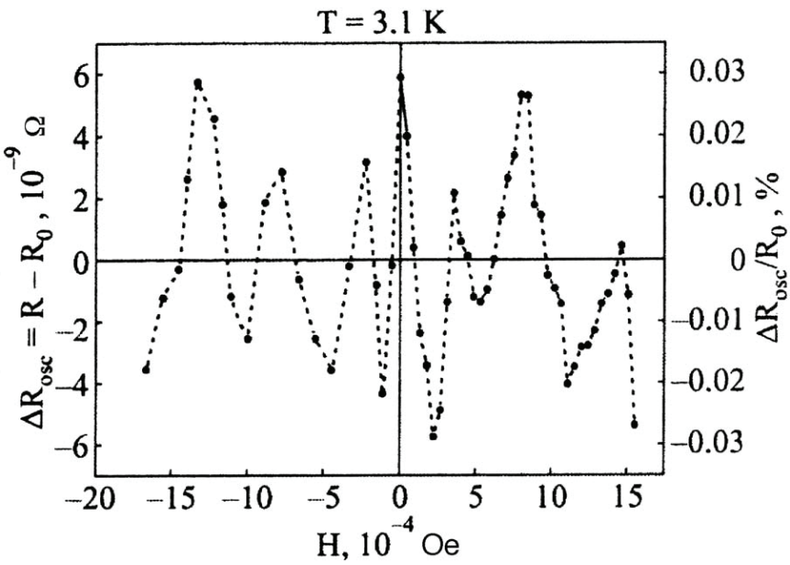


Fig. 17. The $hc/2e$ magnetic-field oscillations of the resistance of a ferromagnetic (Ni) conductor in an AI system with the dimensions given in Fig. 16, in absolute (left-hand scale) and relative (right-hand scale) units. $R_0 = 4.12938 \times 10^{-5}$ Ohm. $T = 3.1$ K.

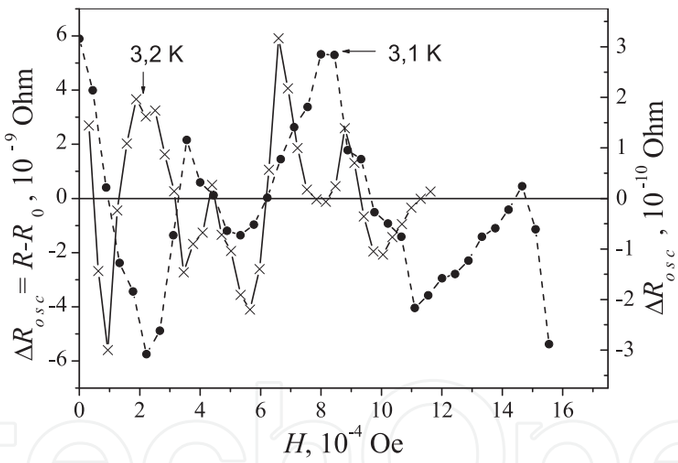


Fig. 18. The $hc/2e$ magnetic-field oscillations of the resistance of a ferromagnetic (Ni) conductor in an AI system with an aperture area twice that of the system illustrated in Fig. 16 (solid curve, right-hand scale). $R_0 = 3.09986 \times 10^{-6}$ Ohm. $T = 3.2$ K. The dashed curve shows the oscillations presented in Fig. 17.

superconductor at the interfaces. Consequently, this parameter should be related to the diffusion trajectories of the electrons on which the "phase memory" is preserved within the whole length L of the ferromagnetic segment. This means that the oscillations are observed in the regimes $L \leq L_\varphi = \sqrt{D\tau_\varphi} \gg \xi_T$ (D is the diffusion coefficient, ξ_T is the coherence length of the metal, over which the proximity effect vanishes, and τ_φ is the dephasing time). It is well known that the possibility for the Aharonov-Bohm effect to be manifested under these

conditions was proved by Spivak and Khmelnitskii (Spivak & Khmelnitskii, 1982), although the large value of L_φ coming out of our experiments is somewhat unexpected.

3.2.1 The entanglement of Andreev hybrids

The estimated value of L_φ raises a legitimate question of the nature of the observed effect and the origin of the dephasing length scale evaluated. Since, as discussed in the Introduction, L_φ is determined by the scale of the inelastic mean free path, the main candidates for the mechanism of inelastic scattering of electrons in terms of their elastic scattering on impurities remain electron-electron ($e-e$) and electron-phonon ($e-ph$) interactions.

Direct measurement of the temperature-dependent resistance of the ferromagnetic (Ni) segment in the region below T_c^{In} found that $(\delta R_{e-ph}/R_{el}) \sim (l_{el}/l_{e-ph}) \approx 10^{-3} - 10^{-4}$. It follows that for our Ni segment with $l_{el} > 10^{-3}$ cm and $D \sim 10^5$ cm^2/s, the electron-phonon relaxation time should be $\tau_{e-ph} \sim (10^{-7} - 10^{-8})$ s, which value coincides, incidentally, with the semiclassical estimate $\tau_{e-ph} \sim (\hbar/T)(T_{\mathrm{D}}/T)^4$ (T_{D} is the Debye temperature). On the other part, $\tau_{e-e} \sim \hbar\mu_e/T^2$ (μ_e is the chemical potential) at 3 K has the same order of magnitude. Thereby, the dephasing length in the studied systems can have a macroscopical scale of the order of $L_\varphi = \sqrt{D\tau_\varphi} \sim 1$ mm, which corresponds to the length of F segments of our interferometers.

Under these conditions the nature of the observed oscillations can be assumed as follows. According to the arguments offered by Spivak and Khmelnitskii (Spivak & Khmelnitskii, 1982), in a metal, regardless of the sample geometry (the parameters $L_{x,y,z}$), there always exists a finite probability for the existence of constructively interfering transport trajectories, the oscillatory contribution of which does not average out. Such trajectories coexist with destructively interfering ones, the contributions from which average to zero. An example would be the Sharvin's experiment (Sharvin & Sharvin, 1981). In the doubly connected geometry, the probability for the appearance of trajectories capable of interfering constructively increases.

Consider the model shown in Fig. 19. Cooper pairs injected into the magnetic segment are split due to the magnetization and lose their spatial coherence over a distance $\xi^* = \sqrt{2\lambda_{\mathrm{B}} r_{\mathrm{exch}}}$ from the interface (see Sec. 3. 1. 1). r_{exch} is the Larmor radius in the exchange field $H_{\mathrm{exch}} \approx k_{\mathrm{B}}T_{\mathrm{C}}$; $r_{\mathrm{exch}} \sim 1$ μm. (Recall that ξ^* is the distance at which simultaneous interaction of e and h quasiparticles with the same impurity is still admissible.)

The phase shifts acquired by (for example) an electron *3* and hole *2* on the trajectories connecting the interfaces are equal, respectively, to

$$\begin{aligned} \phi_e &= (k_{\mathrm{F}} + \varepsilon_T/\hbar v_{\mathrm{F}})L_e + 2\pi\Phi/\Phi_0 = \phi_{0e} + 2\pi\Phi/\Phi_0, \\ \phi_h &= -(k_{\mathrm{F}} - \varepsilon_T/\hbar v_{\mathrm{F}})L_h + 2\pi\Phi/\Phi_0 = \phi_{0h} + 2\pi\Phi/\Phi_0. \end{aligned} \tag{24}$$

Here ε_T and k_{F} are the energy, measured from the Fermi level and the modulus of the Fermi wave vector, respectively. Since the trajectories of an $e-h$ pair are spatially incoherent, their oscillatory contributions, proportional to the squares of the probability amplitudes, should combine additively:

$$|f_{h(2)}|^2 + |f_{e(3)}|^2 \sim \cos\phi_h + \cos\phi_e \sim \cos(\phi_0 + 2\pi\Phi/\Phi_0), \tag{25}$$

where ϕ_0 is the relative phase shift of the independent oscillations, equal to

$$\phi_0 = (1/2)(\phi_{0e} + \phi_{0h}) \approx (\varepsilon_T/\varepsilon_L)(L_e + L_h)/2L, \tag{26}$$

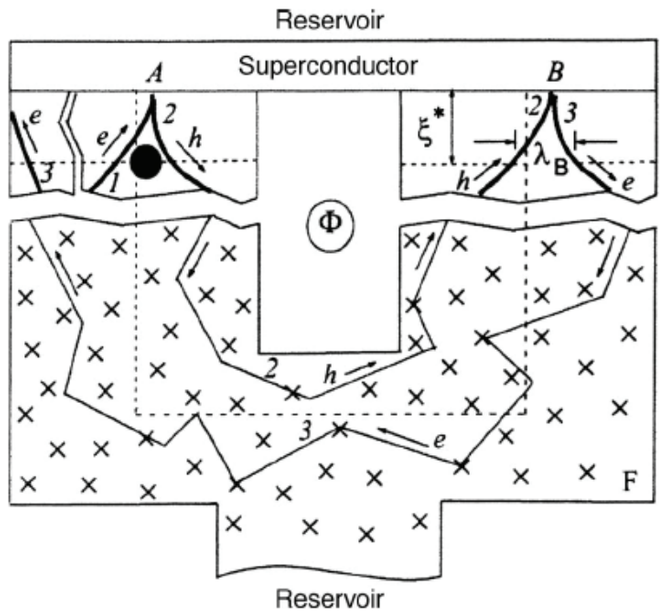


Fig. 19. Geometry of the model.

where $\varepsilon_L = \hbar v_F/L$; $\varepsilon_T = k_B T = \hbar D/\xi_T^2$. Hence it follows that any spatially separated e and h diffusion trajectories with $\phi_0 = 2\pi N$, where N is an integer, can be phase coherent. Clearly this requirement can be satisfied only by those trajectories whose midlines along the length coincide with the shortest distance L connecting the interfaces. In this case, $(L_e + L_h)/2L$ is an integer, since $L_{i(e,h)}, L \propto l_{el}$ and $(L_{i(e,h)}/L) = m(1+\alpha)$, where $\alpha \ll 1$. Furthermore, $(\varepsilon_T/\varepsilon_L)/2\pi$ is also an integer n to an accuracy of $n(1+\gamma)$, where $\gamma \approx (d/L) \ll 1$ (d is the transverse size of the interface). In sum, considering all the foregoing we obtain

$$\cos(\phi_0 + 2\pi\Phi/\Phi_0) \sim \cos(2\pi\Phi/\Phi_0). \tag{27}$$

This means that the contributions oscillatory in magnetic field from all the trajectories should have the same period. Taking into consideration the quasiclassical thickness of a trajectory, we find that the number of constructively interfering trajectories with different projections on the quantization area, those that must be taken into account, is of the order of (l_{el}/λ_B). However, over the greater part of their length, except for the region ξ^*, all (l_{el}/λ_B) trajectories are spatially incoherent. They lie with equal probability along the perimeter of the cross section of a tube of radius l_{el} and axis L, and therefore outside the region ξ^* they average out. Constructive interference of particles on these trajectories can be manifested only over the thickness of the segment ξ^*, reckoned from the interface, where the particles of the $e-h$ pairs are both phase- and spatially coherent. In this region the interaction of pairs with an impurity, as mentioned in the Introduction, leads to a resistive contribution. When the total length of the trajectories is taken into account, the value of this contribution for one pair should be of the order of ξ^*/L. Accordingly, one can expect that the amplitude of the constructive oscillations will have a relative value of the order of

$$\delta R^{\xi^*}/R_L \approx (\xi^*/L)(l_{el}/l_{el}^{\xi^*}) \sim l_{el}^L/L, \tag{28}$$

($l_{el}^{\xi^*} \sim \lambda_B$, see sec. 2.1.1), i. e., the same as the value of the effect measured with the superconducting bridge open. Our experiment confirms this completely: For the samples

with the oscillations shown in Figs. 17 and 18, $\delta R^{\tilde{\xi}^*}/R_L \approx 0.03\%$ and 0.01%, respectively. This is much larger than the total contribution from the destructive trajectories, which in the weak-localization approximation is of the order of $(\lambda_B/l_{el})^2$ and which can lead to an increase in the conductance (Altshuler et al., 1981). One should also note that the property of the oscillations under discussion described by Eq. (27) presupposes that the resistance for $H = 0$ will decrease as the field is first introduced, and this, as can be seen in Figs. 17 and 18, agrees with the experiment.

4. Conclusion

Here, we presented the results of the study of Andreev reflection in a macroscopic formulation of experiments, consisting in increasing simultaneously the diffusion coefficient in normal segments of NS hybrid systems and the size of these segments by a factor of $10^3 - 10^4$ as compared with those characteristics of mesoscopic systems. Our data prove that at temperatures below 4 K, the relaxation of the electron momentum, at least at sufficiently rare collisions of electrons with static defects, are not accompanied by a break of the phase of electron wave functions. Hence, the electron trajectories in the classical approximation may be reversible on a macroscopic length scale of the order of several millimeters, both in a nonmagnetic and in a sufficiently pure ferromagnetic metal. In this situation, there appears a possibility to observe conductance oscillations in doubly connected NS systems in Andreev-reflection regime, with a period $hc/2e$ in a magnetic field, which indicates that the interference occurs between singlet bound quasiparticles rather than between triplet bound electrons, as in the Aharonov-Bohm ring. With the current flowing perpendicular to the $N(F)S$ interfaces in singly connected samples, a nonequilibrium resistive contribution of the interfaces was found. We associate this with the spin polarization of a certain region of a ferromagnet under the interface. The observed increase in the resistance corresponds to the theoretically predicted magnitude of the change occurring in the resistance of a single-domain region with spin-polarized electrons as a result of spin accumulation at the F/S interface under the conditions of limiting Andreev reflections.

5. References

Aharonov, Y. & Bohm, D. (1959). Significance of electromagnetic potentials in the quantum theory. *Phys. Rev.*, Vol. 115, No. 3, (1959) 485-491.

Altshuler, B. L., Aronov, A. G. , & Spivak, B. Z. (1981). The Aharonov-Bohm effect in disordered conductors. *JETP Lett.*, Vol. 33, No. 2, (1981) 94-97.

Altshuler, B. L., Khmelnitsky, D. E., Larkin, A. I., et al. (1980). Magnetoresistance and Hall effect in a disordered two-dimensional electron gas. *Phys. Rev. B*, Vol. 22, No. 11, (1980) 5142-5153.

Andreev, A. F. (1964). Thermal conductivity of the intermediate state of superconductors. *Sov. Phys. JETP*, Vol. 19, No. 6, (1964)1228-1234.

Aronov, A. G. & Sharvin, Yu. V. (1987). Magnetic flux effects in disordered conductors. *Rev. Mod. Phys.*, Vol. 59, No. 3, (1987) 755-779.

Belzig, W., Brataas, A., Nazarov, Yu. V., et al. (2000). Spin accumulation and Andreev reflection in a mesoscopic ferromagnetic wire. *Phys. Rev. B*, Vol. 62, No. 14, (2000) 9726-9739.

Blonder, G. E., Tinkham, M., & Klapwijk, T. M. (1982). Transition from metallic to tunneling regimes in superconducting microconstrictions: Excess current, charge imbalance, and supercurrent conversion. *Phys. Rev. B*, Vol. 25, No. 7, (1982) 4515-4532.

Chiang, Yu. N. (1985). Superconducting modulator of the measuring circuit conductance over a wide range of helium temperatures. *Prib. Tekhn. Eksp.*, No. 1, (1985) 202-204.

Chiang, Yu. N. & Shevchenko, O. G. (1988). Measurement of resistance of the normal metal-superconductor (N-S) boundary. *Sov. J. Low Temp. Phys.*, Vol. 14, No. 5, (1988) 299-301.

Chiang, Yu. N. & Shevchenko, O. G. (1998). Contribution of Andreev reflection to the increase in the resistance of the normal metal in a bimetallic N-S structure. *JETP*, Vol. 86, No. 3, (1998) 582-585.

Chiang, Yu. N. & Shevchenko, O. G. (1999). Conductivity of normal metal with phase-coherent excitations in the presence of NS boundary. *Low Temp. Phys.*, Vol. 25, No. 5, (1999) 314-326.

Chiang, Yu. N. & Shevchenko, O. G. (2001). Mesoscopic quantum scillations of the resistance in the intermediate state of type-I superconductors. *Low Temp. Phys.*, Vol. 27, No. 12, (2001) 1000-1009.

Chiang, Yu. N., Shevchenko, O. G., & Kolenov, R. N. (2007). Manifestation of coherent and spin-dependent effects in the conductance of ferromagnets adjoining a superconductor. *Low Temp. Phys.*, Vol. 33, No. 4, (2007) 314-320.

Clarke, J., Eckern, U. , Schmid, A., et al. (1979). Branch-imbalance relaxation times in superconductors. *Phys. Rev. B*, Vol. 20, No. 9, (1979) 3933-3937.

Falko, V. I., Volkov, A. F., & Lambert, C. J. (1999). Andreev reflections and magnetoresistance in ferromagnet-superconductor mesoscopic structures. *JETP Lett.*, Vol. 69, No. 7, (1999) 532-537.

De Gennes, P. G. (1966). *Superconductivity of Metals and Alloys* , W.A. Benjamin, New York.

Giroud, M., Hasselbach, K., Courtois, H., et al. (2003). Electron transport in a mesoscopic superconducting/ferromagnetic hybrid conductor. *Eur. Phys. J. B*, Vol. 31, No. 1, (2003) 103-109.

Gueron, S., Pothier, H., Birge, N. O. et al. (1996). Superconducting proximity effect probed on a mesoscopic length scale. *Phys. Rev. Lett.*, Vol. 77, No. 14, (1996) 3025-3028.

Handbook of Chemistry and Physics, Chem. Pub., Cleveland.

Herath, J. & Rainer, D. (1989). Effects of impurities on Andreev reflection in an NS bilayer. *Physica C*, Vol. 161, No. 2, (1989) 209-218.

Hofstetter, L., Csonka, S., Nygard, J., et al. (2009). Cooper pair splitter realized in a two-quantum-dot Y-junction. *Nature*, Vol. 461, No. 10, (2009) 960-963.

Hsiang, T. Y. & Clarke, J. (1980). Boundary resistance of the superconducting - normal interface. *Phys. Rev. B*, Vol. 21, No. 3, (1980) 945-955.

Jedema, F. J., van Wees, B. J., Hoving, B. H., et al. (1999). Spin-accumulation-induced resistance in mesoscopic ferromagnet/superconductor junctions. *Phys. Rev. B*, Vol. 60, No. 24, (1999) 16549-16552.

Jin, B. Y. & Ketterson, J. B. (1989). Artificial metallic superlattices. *Adv. Phys.*, Vol. 38, No. 3, (1989) 189-366.

De Jong, M. J. M. & Beenakker, C. W. J. (1995). Andreev reflection in ferromagnet-superconductor junctions. *Phys. Rev. Lett.*, Vol. 74, No. 9, (1995) 1657-1660.

Kadigrobov, A. M. (1993). Multiple electron scattering by an impurity and at the NS boundary. Negative differential conductivity of the NSN system. *Low Temp. Phys.*, Vol. 19, No. 8, (1993) 671-672.

Kadigrobov, A., Zagoskin, A., Shekhter, R. I., et al. (1995). Giant conductance oscillations controlled by supercurrent flow through a ballistic mesoscopic conductor. *Phys. Rev. B*, Vol. 52, No. 12, (1995) R8662-R8665.

Kulik, I. O. (1969). Macroscopic quantization and proximity effect in S-N-S junctions. *Sov. Phys. JETP*, Vol. 30, No. 5, (1969) 944-958.

Lambert, C. J. & Raimondi, R. (1998). Phase-coherent transport in hybrid superconducting nanostructures. *J. Phys.: Condens. Matter*, Vol. 10, (1998) 901-941.

Landauer, R. (1970). Electrical resistance of disordered one-dimensional lattices. *Phil. Mag.*, Vol. 21, No. 172, (1970) 863-867.

Lifshitz, E. M. & Sharvin, Yu. V. (1951). On the intermediate state of superconductors. *Dokl. Akad. Nauk Ukr. SSR*, Vol. 79, No. 5, (1951) 783-786.

Petrashov, V. T., Sosnin, I. A., Cox, I., et al. (1999). Giant mutual proximity effects in ferromagnetic/superconducting nanostructures. *Phys. Rev. Lett.*, Vol. 83, No. 16, (1999) 3281-3284.

Sharvin, D. Yu. & Sharvin, Yu. V. (1981). Magnetic flux quantization in a cylindrical film of a normal metal. *JETP Lett.*, Vol. 34, No. 5, (1981) 272-275.

Soulen, R. J., Jr., Byers, J. M., Osofsky, M. S., et al. (1998). Measuring the spin polarization of a metal with a superconducting point contact. *Science*, Vol. 282, No. 5386, (1998) 85-88.

Spivak, B. Z. & Khmelnitskii, D. E. (1982). Influence of localization effects in a normal metal on the properties of SNS junction. *JETP Lett.*, Vol. 35, No. 8, (1982) 412-416.

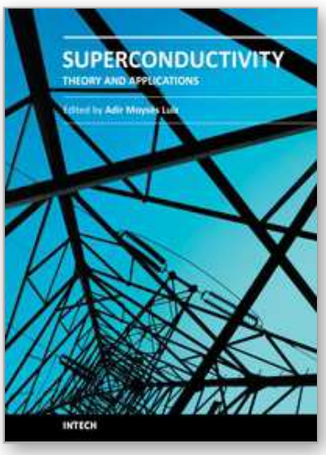
Tsyan (Chiang), Yu. N. (2000). Resistance quantum oscillations in the intermediate state of singly connected Pb and Sn samples. *JETP Lett.*, Vol. 71, No. 8, (2000) 334-337.

Washburn, S. & Webb, R. A. (1986). Aharonov-Bohm effect in normal metal. Quantum coherence and transport. *Adv. Phys.*, Vol. 35, No. 4, (1986) 375-422.

Van Wees, B. J., de Vries, P., Magnic, P., et al. (1992). Excess conductance of superconductor-semiconductor interfaces due to phase conjunction between electrons and holes. *Phys. Rev. Lett.*, Vol. 69, No. 3, (1992) 510-513.

Zhou, F., Spivak, B., & Zyuzin, A. (1995). Coherence effects in a normal-metal-insulator-superconductor junction. *Phys. Rev. B*, Vol. 52, No. 6, (1995) 4467-4472.

IntechOpen



Superconductivity - Theory and Applications
Edited by Dr. Adir Luiz

ISBN 978-953-307-151-0
Hard cover, 346 pages
Publisher InTech
Published online 18, July, 2011
Published in print edition July, 2011

Superconductivity was discovered in 1911 by Kamerlingh Onnes. Since the discovery of an oxide superconductor with critical temperature (Tc) approximately equal to 35 K (by Bednorz and Müller 1986), there are a great number of laboratories all over the world involved in research of superconductors with high Tc values, the so-called â€œHigh-Tc superconductorsâ€. This book contains 15 chapters reporting about interesting research about theoretical and experimental aspects of superconductivity. You will find here a great number of works about theories and properties of High-Tc superconductors (materials with Tc > 30 K). In a few chapters there are also discussions concerning low-Tc superconductors (Tc < 30 K). This book will certainly encourage further experimental and theoretical research in new theories and new superconducting materials.

How to reference
In order to correctly reference this scholarly work, feel free to copy and paste the following:

Yurii Tszyan (Chiang) (2011). Electronic transport in an NS system with a pure normal channel. Coherent and spin-dependent effects, Superconductivity - Theory and Applications, Dr. Adir Luiz (Ed.), ISBN: 978-953-307-151-0, InTech, Available from: http://www.intechopen.com/books/superconductivity-theory-and-applications/electronic-transport-in-an-ns-system-with-a-pure-normal-channel-coherent-and-spin-dependent-effects

INTECH
open science | open minds

InTech Europe
University Campus STeP Ri
Slavka Krautzeka 83/A
51000 Rijeka, Croatia
Phone: +385 (51) 770 447
Fax: +385 (51) 686 166
www.intechopen.com

InTech China
Unit 405, Office Block, Hotel Equatorial Shanghai
No.65, Yan An Road (West), Shanghai, 200040, China
中国上海市延安西路65号上海国际贵都大饭店办公楼405单元
Phone: +86-21-62489820
Fax: +86-21-62489821

© 2011 The Author(s). Licensee IntechOpen. This chapter is distributed under the terms of the Creative Commons Attribution-NonCommercial-ShareAlike-3.0 License, which permits use, distribution and reproduction for non-commercial purposes, provided the original is properly cited and derivative works building on this content are distributed under the same license.

IntechOpen

IntechOpen